

speed [13]. Thus, qPCR is very useful for investigating physiological and pathological status from a small amount of sample. Normalization to reference genes such as housekeeping genes is usually required for qPCR analysis. However, expression levels of reference genes may vary between tissues, cell types and experimental conditions. Therefore, the validation of suitable reference genes in each experiment is critical for the accurate evaluation of qPCR data. Recently, a set of guidelines for evaluating qPCR experiments was developed [14] and a strict method for the selection of reference genes suitable for normalization was proposed [15]. A freely available program, *geNorm* applet (<http://medgen.ugent.be/~jvdesomp/genorm/>), can determine gene stability ranking and the number of reference genes required for normalization in a given panel of samples [15].

To develop an accurate and reliable qPCR method for common marmosets, we examined the expression stabilities of candidate reference genes in various tissues of laboratory common marmosets using *geNorm* applet. Then, we compared expression levels of immune-related genes in peripheral blood leukocytes between common marmosets and humans. To the best of our knowledge, this is the first such study for the selection of reference genes in common marmosets. The present data will contribute to future studies of gene expression analysis by qPCR for common marmosets.

Materials and Methods

Ethics statement

The study was conducted in accordance with the Act on Welfare and Management of Animals of Japanese government. All animals were housed, cared for, and used according to the principles set forth in the Guide for the Care and Use of Laboratory Animals: Eighth Edition (National Research Council, 2011). All experiments using common marmosets were approved by the committee for animal experiments at the National Institute of Infectious Diseases (Approval Number: 610,007). For humans, whole blood was obtained from eight healthy volunteers (mean age \pm sd: 35.7 \pm 13.0 years old) after obtaining written informed consent. This study and the consent procedure were approved by the ethics committee of Tokai University School of Medicine (Approval Number: 10I-22).

Animals

Eight common marmosets (1.58 \pm 0.29 years old) were obtained from CLEA Japan, Inc. (Tokyo, Japan) and maintained in specific pathogen-free conditions at the National Institute of Infectious Diseases (Tokyo, Japan). Common marmosets were housed solely or in pairs in a single cages 39 cm (W) \times 55 (D) \times 70 (H) in size on 12:12 h light/dark cycles. Room temperature and humidity were maintained at 26–27°C and 40–50%, respectively. Filtered drinking water was delivered by an automatic watering system and total 40–50 g/individual of commercial marmoset chow (CMS-1M, CLEA Japan) were given in a couple of times per day. Dietary supplements (sponge cakes, eggs, banana pudding, honeys, vitamin C and D3) were also given to improve their health status. Machinery noise and dogs' barks were avoided to reduce stress. The cages were equipped with resting perches and a nest box as environmental enrichment. The marmosets were routinely tested to assure the absence of pathogenic bacteria, viruses, and parasite eggs in the animal facilities and did not exhibited abnormal external appearances. Four common marmosets were euthanized by cardiac exsanguinations under anesthesia with Ketamine hydrochloride (50 mg/kg, IM) and Xylazine (3.0 mg/kg, IM).

After sacrifice, various tissues removed, and whole blood was obtained from all eight common marmosets.

RNA isolation

Heparinized venous blood samples from common marmosets were obtained before sacrifice and incubated in erythrocyte lysis buffer (155 mM NH₄Cl, 10 mM KHCO₃, and 0.1 mM EDTA). Following incubation on ice for 5 min, cells were centrifuged at 300 \times g for 10 min at 4°C and washed with lysis buffer and then PBS. Leukocytes were lysed with QIAzol[®] Lysis Reagent (Qiagen, Hilden, Germany) and total RNA was extracted using an RNeasy[®] Plus Universal Mini Kit (Qiagen) according to the manufacturer's instructions. Tissue samples (spleen, mesenteric lymph node, jejunum, ileum, descending colon, cerebrum, cerebellum, brainstem, heart, lung, liver and kidney) were excised from each animal and immediately submerged in RNAlater[®] RNA Stabilization Reagent (Qiagen). Then total RNA was extracted using RNeasy[®] Plus Universal Mini Kit (Qiagen). RNA concentration and integrity were assessed using the Agilent RNA 6,000 Nano Kit (Agilent Technologies, Inc., CA, USA) in an Agilent 2100 Bioanalyzer. All RNA samples were confirmed to have no degradation and were of optimal quality for downstream qPCR applications.

Candidate reference genes

Based on a literature search, eight commonly used candidate internal control genes were selected for analysis: *GAPDH* (glyceraldehyde-3-phosphate dehydrogenase), *ACTB* (actin, beta), *rRNA* (18S ribosomal RNA), *B2M* (beta-2-microglobulin), *UBC* (ubiquitin C), *HPRT* (hypoxanthine phosphoribosyltransferase 1), *SDHA* (succinate dehydrogenase complex, subunit A) and *TBP* (TATA-box binding protein). All genes chosen have independent cellular functions and are not thought to be co-regulated. The sequences of primers specific for each reference gene are shown in Table 1.

Quantitative real-time PCR

First-strand cDNA was synthesized using PrimeScript[®] RT reagent Kit (Takara Bio, Otsu, Japan) with attached random hexamers and oligo(dT) primers. Reactions were incubated at 37°C for 15 min followed by 85°C for 5 sec according to the manufacturer's instructions. Then each cDNA sample was diluted with RNase/DNase-free water to 25 ng/ μ L. The expression level of each gene was analyzed by qPCR using the Bio-Rad CFX96 system (Bio-Rad Laboratories, Inc., Hercules, CA, USA). PCR reactions consisted of 5 μ L of SsoFast[™] EvaGreen[®] Supermix (Bio-Rad), 3.5 μ L of RNase/DNase-free water, 0.5 μ L of 5 μ M primer mix, 1 μ L of cDNA in a total volume of 10 μ L. The primer sequences are shown in Tables 1 and 2. Cycling conditions were as follows: 30 sec at 95°C followed by 45 rounds of 95°C for 1 sec and 60°C for 5 sec. Melting curve analysis to determine the dissociation of PCR products was performed between 65°C and 95°C. Data were expressed as mean values of experiments performed in triplicate. Seven points of a 10-fold serial dilution of standard DNA was used for absolute quantification. Standard DNA was generated by cloning PCR products into pGEM-T Easy Vector (Promega, WI, USA). Sequences of the cloned plasmid were confirmed by DNA sequencing using the CEQ8000 Genetic Analysis System (Beckman Coulter). Quality and concentration of the plasmid DNA were validated using Agilent DNA 7,500 Kit in an Agilent 2100 Bioanalyzer.

Table 1. Sequences of qPCR primers for housekeeping genes.

Target gene	Species	5'-primer sequence -3 ^(a),b)		Product size (bp)	PCR efficiency	Reference
		Forward	Reverse			
GAPDH	Cj	TCGGAGTCAACGGATTTGGTC	TTCCCCTTCTCAGCCTTGAC	181	0.920	DD279474
	Hs	-----	-----	181	0.921	AF261085
ACTB	Cj	GATGGTGGGCATGGGTCAGAA	AGCCACACGCAGCTCGTTGT	163	0.901	DD279463
	Hs	-----	-----A----	163	0.883	NM_0011101
HPRT	Cj	ATCCAAAGATGGTCAAGGTCG	GTATTCATTATAGTCAAGGGCATA	134	0.842	DD289567
	Hs	-----	-----	134	0.880	M31642
B2M	Cj	CTATTCAGCATGCTCCAAAGA	AAGACAAGTCTGAATGCTCCAC	168	0.928	AF084623
	Hs	----C----G-A-----	-----	168	0.950	AB021288
UBC	Cj	TCCCTTCTCGGCGGTTCTG	. TGCATTGTCAAGCGGCAT	158	0.922	AB571242
	Hs	-----A-----	TC-----T-A-----	160	0.936	NM_021009
rRNA	Cj	CGACCATAAACGATGCCGAC	GGTGGTGCCCTTCCGTC AAT	145	0.918	AB571241
	Hs	-----	-----	145	0.940	M10098
SDHA	Cj	TGGGAACAAGAGGGCATCTG	CCACCACGGCATCAAATTCATG	86	0.934	XM_002745154
	Hs	-----	-----T-----	86	0.948	BC001380
TBP	Cj	CCATGACTCCCAGGAATCCCTAT	ATAGGCTGTGGGGTCAGTCCA	70	0.920	EU796973
	Hs	-----	-----	70	0.954	M55654

^{a)}Hyphen indicates a nucleotide identical to human sequences.

^{b)}Dot indicates a shift nucleotide to marmoset sequences.

doi:10.1371/journal.pone.0056296.t001

Analysis of gene expression stability

The expression stability of selected reference genes was evaluated using a publicly available program, *geNorm* applet [15]. *geNorm* calculates the stability of tested reference genes according to the similarity of their expression profiles by pairwise comparison and M value, where the gene with the highest value is the least stable one. It is possible to perform sequential elimination of the least stable gene in any given experimental group, thus resulting in the exclusion of all but the two most stable genes in each case.

Flow cytometry

Heparinized peripheral blood was collected from common marmosets and centrifuged in LymphoCept (IBL Co. Takasaki, Japan) at 2,000 rpm for 30 min. Mononuclear cells were collected and re-suspended in RPMI1640 medium containing 10% fetal calf serum. Cells were stained with anti-common marmoset CD8 antibody (Mar8-10) [16] for 15 min at 4°C and washed with 1% (w/v) bovine serum albumin-containing PBS. Subsequently, cells were stained with phycoerythrin-labeled secondary antibody, peridinin chlorophyll protein cyanin5.5 (PerCPCy5.5)-conjugated anti-human CD3 (SP34-2) and Alexa488-conjugated anti-common marmoset CD4 (Mar4-33) antibodies [16]. Peripheral blood from healthy human volunteers was collected and mononuclear cells isolated by Ficoll-Paque (GE Healthcare Biosciences, Uppsala, Sweden) gradient centrifugation. The monoclonal antibodies used for cell staining were as follows: PerCPCy5.5-conjugated anti-human CD3 (SP34-2), allophycocyanin-conjugated anti-human CD4 (SK3), fluorescein isothiocyanate-conjugated anti-human CD8 (HIT8a) (BD PharMingen). Cells were analyzed by FACSCalibur (Becton Dickinson, Franklin Lakes, NJ, USA).

Statistical analysis

Student's *t*-test was used for statistical analysis to assess significant differences in qPCR assays. A *P* value < 0.05 was considered to be statistically significant.

Results

The expression levels of candidate reference genes in tissues

Eight housekeeping genes were chosen as reference genes: *GAPDH*, *ACTB*, *rRNA*, *B2M*, *UBC*, *HPRT*, *SDHA* and *TBP*. We determined the transcription levels of these eight genes in 13 tissues (leukocyte, spleen, lymph node, jejunum, ileum, colon, cerebrum, cerebellum, brainstem, heart, lung, liver and kidney) from four individual common marmosets by qPCR. The sequences of primers specific for each reference gene are shown in Table 1. The expression level of each gene in each tissue is shown as the copy number per µg of purified total RNA (Figure 1). The most abundant gene was *rRNA* while the rarest gene was *UBC* and the difference in expression level between the two genes was more than 100,000-fold. For several genes, the expression levels were highly different among tissues. For example, *B2M* expression in heart and brain segments (cerebrum, cerebellum and brainstem) was markedly lower than in other tissues. *HPRT* expression also showed a large variability among tissues. In addition, the expression levels of *rRNA*, *B2M* and *HPRT* varied among individuals; the mean values of standard deviation were 0.224, 0.235 and 0.303, respectively, while those of the other genes were below 0.2.

Table 2. Sequences of qPCR primers for CD markers and cytokines.

Target gene	Species	5'-primer sequence -3' ^(a), b)		Product size (bp)	PCR efficiency	Reference
		Forward	Reverse			
CD3e	Cj	GGCTTGCTGCTGCTGGTTAC	CCGGATGGGCTCATAGTCTG	150	0.865	DQ189218
	Hs	-----	-----	150	0.848	NM_000733
CD4	Cj	GGAAAACGGGAAAGTTGCATCA	GCCTTCTCCCGCTTAGAGAC	163	0.926	AF452616
	Hs	C-----A-----	-----C-----	162	0.907	M35160
CD8 α	Cj	TCTCCCAAACCAAGTCCAAGG	AGTTTCTCAGGGCCGAGCAG	144	0.940	DQ189217
	Hs	-----A---C-----	. ---G-----	143	0.912	NM_001768
CD20	Cj	GGGCTGTCCAGATTATGAATG	GAGTTTTTCTCCGTTGCTGC	166	0.942	DQ189220
	Hs	-----	-----	166	1.002	X07203
IL-1 β	Cj	TGCACCTGTACGATCCCTGAAC	TTGCACAAAGGACATGGAGAACAC	145	0.806	AB539804
	Hs	-----A-----	---T-----	145	0.780	NM_000576
IL-2	Cj	CCCAAGAAGGCCAAAGAATTG	CTTAAGTGAAGTTTTGCTTTGAG	104	0.773	DQ826674
	Hs	-----C---C--	-----	103	0.797	BC070338
IL-4	Cj	CATTGTCACAGAGCAAAGACTC	CTCAGTTGTGTTCTTGAGGCA	79	0.910	XM_002744606
	Hs	. GCC-----G-----	-----	77	0.878	NM_000589
IL-5	Cj	AATCACCACCTGTGCACTGAAGAA	. TTTGGCGTCAATGTGTTCCCTT	130	0.871	DQ658152
	Hs	-----	TT-----C-----A--T---	132	0.860	NM_000879
IL-6	Cj	GATTCAATGAGGAGACTTGCC	TGTTCTGGAGGTACTCTAGGTA	81	0.920	DQ658153
	Hs	-----	-----	81	0.990	NM_00600
IL-10	Cj	CTGCCTCACATGCTTCGAGA	TGGCAACCAGGTAACCCCTTA	134	0.970	DQ658154
	Hs	-----A-----	-----	134	0.920	M57627
IL-12 β	Cj	. GGACGGCAAGGAGTATGAGTA	TTGAGCTTGTGAACGGCATC	111	0.935	AB539805
	Hs	G---AA-----	-----	112	0.900	M65272
IL-13	Cj	TCCAGCTTGCTTGTCCGAG	CTGCAAATAATGATGC GTT-GATGT	127	0.916	AB571243
	Hs	-----A-----	. -----T--C--A--	127	0.964	NM_002188
IFN- γ	Cj	GGGTTCTCTTGGCTGTTACTG	TGCTAAGAAAAGAGTTCCATTATC	116	0.838	FJ598593
	Hs	-----	. -C-----	115	0.856	NM_000619
TNF- α	Cj	AGCCTGTAGCCCATGTTGTAG	CTCTCAGCTCCACGCCATTG	102	0.887	DQ520835
	Hs	-----	-----	102	0.817	NM_000594

^{a)}Hyphen indicates a nucleotide identical to human sequences.

^{b)}Dot indicates a shift nucleotide to marmoset sequences.

doi:10.1371/journal.pone.0056296.t002

A variety of gene expression stabilities among tissues

To evaluate the expression stability of selected reference genes, we used a publicly available program, *geNorm* applets. *geNorm* provides a ranking of tested genes based on the reference gene stability measure *M*, which is defined as the average pairwise variation of a particular gene compared with all other control genes. Thus, genes with higher *M* values have greater variations of expression. In addition, assessment of the pairwise variations ($V_{n/n+1}$) between each combination of sequential normalization factors allows identification of the optimal number of reference genes. In the original publication describing *geNorm* [15], a threshold of 0.15 for pairwise variation was established, below which the inclusion of additional reference genes was not necessary.

geNorm analysis produced line plots indicating the mean expression stability *M* of the remaining candidate reference genes in each round of the analysis (Figure 2A and 2B), the pairwise variation *V* (Figure 2C) and ranking of the candidate reference

genes from the least stable to the two most stable genes (Figure 3). The stability score *M* indicated that gene expression in spleen, jejunum and cerebellum were relatively less stable than other tissues (Figure 2A and B). However, all tissues tested exhibited high stabilities, as *M* values were less than 1.5, which was the default limit even when all eight genes were analyzed. According to pairwise variation *V* (Figure 2C), the two most stable genes were sufficient for a stable and valid reference for each tissue analyzed by qPCR because $V_{2/3}$ values were less than 0.15 in all tissues. Jejunum was the most variable tissue with a $V_{2/3}$ value of 0.139. Figure 3 shows ranking of gene expression stability based on *M* values. *GAPDH*, *ACTB*, *SDHA* and *TBP* had higher stability, while *HPRT*, *rRNA* and *B2M* were variable in most tissues. *TBP* in intestinal segments (jejunum, ileum and colon) and *SDHA* in brain segments (cerebrum, cerebellum and brain stem) were particularly stable. *HPRT* ranked as the worst of the eight genes in the 13 tissues tested.

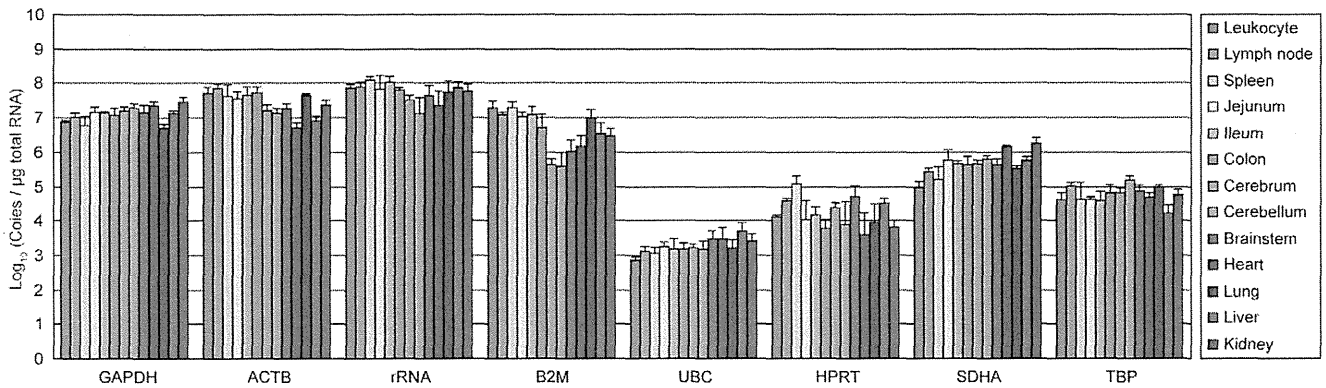


Figure 1. Absolute copy numbers of candidate reference genes. The expression level of each gene in 13 tissues is shown as a logarithmic histogram of absolute copy numbers per μg of total RNA. Means and standard deviations of four individuals are indicated. GAPDH: glyceraldehyde-3-phosphate dehydrogenase; ACTB: actin, beta; rRNA: 18S ribosomal RNA; B2M: beta-2-microglobulin; UBC: ubiquitin C; HPRT: hypoxanthine phosphoribosyltransferase 1; SDHA: succinate dehydrogenase complex, subunit A; TBP: TATA-box binding protein.
doi:10.1371/journal.pone.0056296.g001

Comparison of gene expression levels between human and common marmoset leukocytes

Subsequently, we analyzed gene expression levels of four CD antigens (CD3 ϵ , CD4, CD8 α , and CD20) and ten cytokines,

interleukin (IL)-1 β , IL-2, IL-4, IL-5, IL-6, IL-10, IL-12 β , IL-13, interferon (IFN)- γ and tumor necrosis factor (TNF)- α , in peripheral blood leukocytes from humans and common marmosets (Figure 4). The sequences of primers specific for these

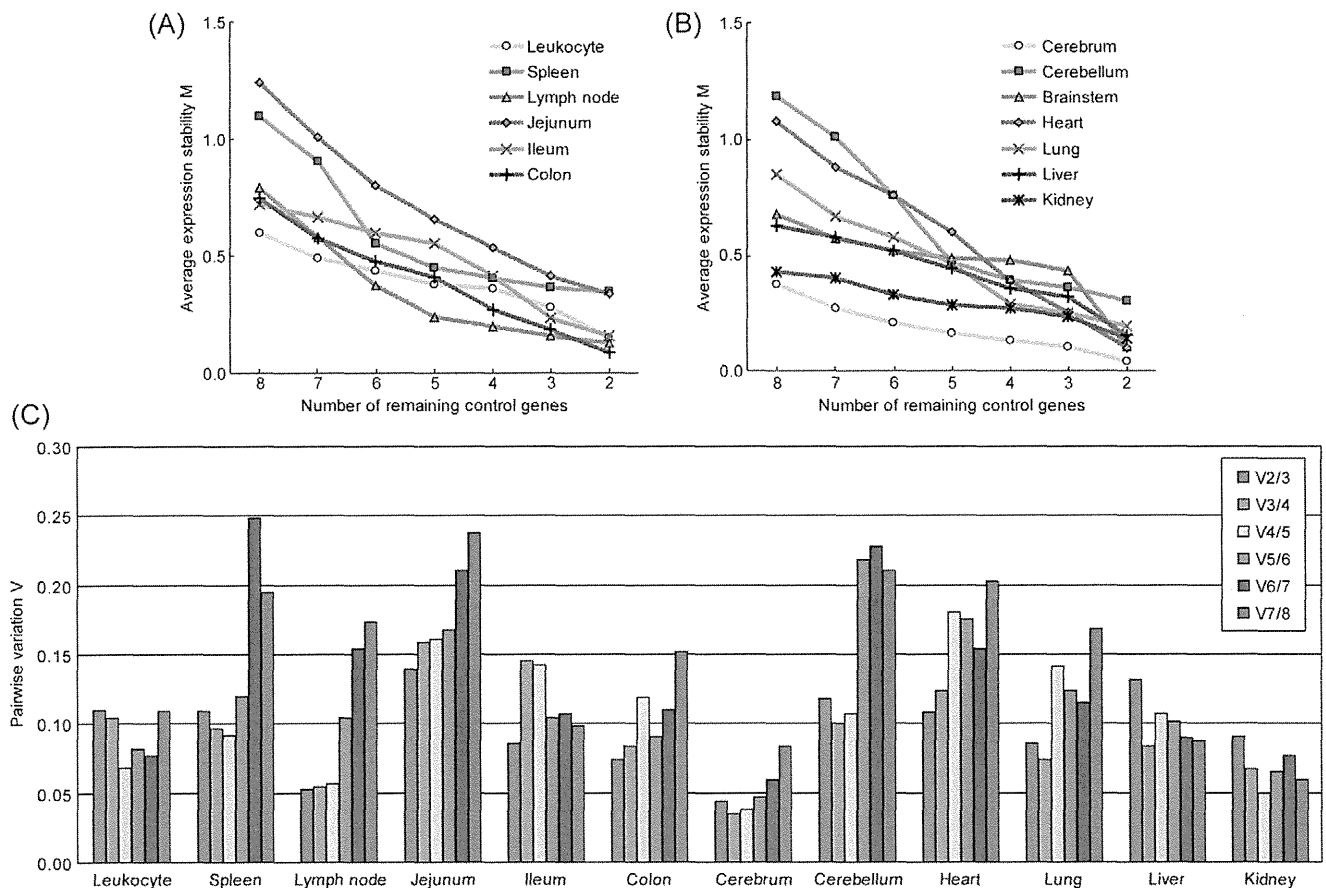


Figure 2. Gene expression stability and pairwise variation of candidate reference genes using *geNorm* analysis. (A) and (B): Average gene expression stability values M of the remaining reference genes during stepwise exclusion of the least stable gene in the different tissue panels are shown. Data are divided into two figures to avoid closely-packed lines. See also figure 3 for the ranking of genes according to their expression stability. (C) Pairwise variation analysis was used to determine the optimal number of reference genes for use in qPCR data normalization. The recommended limit for V value is 0.15, the point at which it is unnecessary to include additional genes in a normalization strategy.
doi:10.1371/journal.pone.0056296.g002

Stability	High							Low
Leukocyte	GAPDH-UBC	ACTB	SDHA	TBP	B2M	rRNA	HPRT	
Spleen	GAPDH-SDHA	ACTB	TBP	UBC	rRNA	B2M	HPRT	
Lymph node	rRNA-TBP	ACTB	SDHA	UBC	GAPDH	B2M	HPRT	
Jejunum	UBC-TBP	GAPDH	B2M	SDHA	ACTB	rRNA	HPRT	
Ileum	B2M-TBP	UBC	ACTB	HPRT	SDHA	GAPDH	rRNA	
Colon	ACTB-TBP	SDHA	GAPDH	rRNA	UBC	HPRT	B2M	
Cerebrum	GAPDH-SDHA	rRNA	ACTB	HPRT	UBC	TBP	B2M	
Cerebellum	SDHA-TBP	GAPDH	ACTB	UBC	rRNA	B2M	HPRT	
Brainstem	ACTB-SDHA	UBC	rRNA	HPRT	GAPDH	TBP	B2M	
Heart	SDHA-TBP	GAPDH	ACTB	UBC	B2M	rRNA	HPRT	
Lung	SDHA-TBP	ACTB	GAPDH	UBC	B2M	rRNA	HPRT	
Liver	GAPDH-SDHA	HPRT	rRNA	ACTB	TBP	UBC	B2M	
Kidney	GAPDH-SDHA	TBP	UBC	ACTB	B2M	rRNA	HPRT	

Figure 3. Ranking of gene expression stability of candidate reference genes using *geNorm* analysis. Candidate reference genes are ranked in order of stability for each tissue with the two most stable genes at the left and the least stable at the right.
doi:10.1371/journal.pone.0056296.g003

immune-related genes are shown in Table 2. The normalization factor for common marmoset leukocytes was calculated using *GAPDH* and *UBC* based on the *geNorm* analysis as described above. For human leukocytes, we found that the expression of all eight genes were stable (M value = 0.363), of which *ACTB* and *HPRT* had the best score (M value = 0.163, $V_{2/3}$ = 0.062) and were selected for use. The expression levels of CD4 and IL-4 were significantly lower in common marmosets than in humans while those of IL-10, IL-12 β and IFN- γ were significantly higher in common marmosets compared with humans. Of interest, the expression level of IL-4 was notably lower in common marmosets than humans, and was close to the detection limit. There was no statistical difference in the expression levels of the other genes tested between common marmosets and humans.

Difference of CD4/CD8 ratio between humans and common marmosets

We calculated ratios of the expression levels of CD4 to CD8 (CD4/CD8 ratio) in human and common marmoset leukocytes (Figure 5, left panel). CD4/CD8 ratios were significantly higher in

human leukocytes compared with common marmoset leukocytes (mean \pm sd, 0.59 ± 0.22 vs. -0.49 ± 0.41 , $P < 0.01$). To confirm the difference in CD4/CD8 ratios, we examined the proportion of CD4 $^{+}$ and CD8 $^{+}$ in CD3 $^{+}$ T cells by flow cytometric analysis. As shown in Figure 6, the rates of CD3 $^{+}$ cells in the lymphocyte gate were similar between common marmosets (30%) and humans (38%). However, the rates of CD4 $^{+}$ /CD3 $^{+}$ cells and CD8 $^{+}$ /CD3 $^{+}$ cells was 36% and 61% in common marmosets, respectively, and 75% and 21% in humans, respectively. Similarly, the CD4/CD8 ratio was markedly different between common marmosets and humans (mean \pm sd, 0.56 ± 0.08 vs. 3.22 ± 0.35 , $P < 0.01$) by qPCR. This indicated a good correlation between the results from FACS analysis and that of qPCR analysis. To examine whether the CD4/CD8 ratio is affected by age, we further performed FACS analyses with PBMCs from young and old marmosets (Table 3). The result showed that the inverted CD4/CD8 ratio was fairly constant among individuals and over ages.

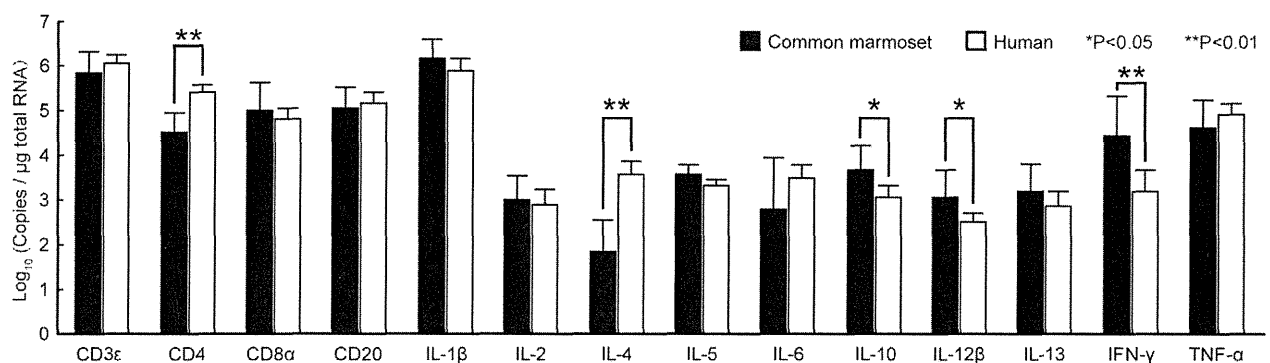


Figure 4. The expression levels of CD antigens and cytokine genes in common marmoset and human leukocytes. The expression level of each gene is shown as a logarithmic histogram of absolute copy numbers per μ g of total RNA. Means and standard deviations of eight individuals are indicated. Asterisk indicates statistically significant differences between marmosets and humans by Student's *t*-test (* P value < 0.05, ** P value < 0.01).
doi:10.1371/journal.pone.0056296.g004

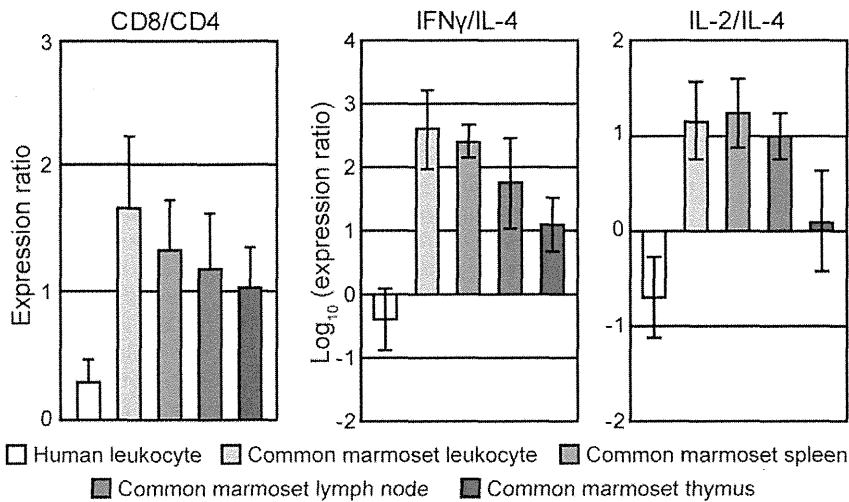


Figure 5. The expression ratios of CD8 to CD4 (CD8:CD4) and Th1-related genes to Th2-related genes. The ratio of CD8:CD4 (left panel), IFN- γ :IL-4 (middle panel) and IL-2:IL-4 (right panel) in human and common marmoset leukocytes, spleen, lymph node and thymus are shown. Significant differences in the CD8:CD4, IFN- γ :IL-4 and IL-2:IL-4 ratios were found between human leukocytes and common marmoset tissues (* $P < 0.05$).

doi:10.1371/journal.pone.0056296.g005

Difference in T helper 1 (Th1)/T helper 2 (Th2) balance between humans and common marmosets

We compared the ratios of expression levels of Th1-related genes (IFN- γ or IL-2) and Th2-related genes (IL-4) (IFN- γ :IL-4 or IL-2:IL-4 ratio) (Figure 5, middle and right panels). Both logarithmic values of the IFN- γ :IL-4 and IL-2:IL-4 ratios were negative in human leukocytes whereas those of common marmoset leukocytes, spleen, lymph node and thymus indicated positive values, showing a clear difference in the Th1/Th2 balance between humans and common marmosets.

Discussion

In the present study, we evaluated the expression stability of common marmoset housekeeping genes in various tissues. To the best of our knowledge, this is the first report of a systematic

evaluation of potential reference genes in common marmosets. We chose eight commonly used classical housekeeping genes. Of all genes tested, *rRNA* showed the most abundant expression and *UBC* showed the lowest expression. The *UBC* gene contains multiple directly repeated ubiquitin coding sequences (i.e., polyubiquitin precursor protein) [17]. However, the primer set we used enabled amplification of the unrepeated sequence at the 5' region of the *UBC* gene only. Thus, low *UBC* expression in our data does not reflect the amount of ubiquitin C protein. *B2M* expression levels were markedly lower in brains and hearts than in other tissues. Resident brain cells normally express few or no MHC class I and B2M molecules [18–20]. In addition, *B2M* expression is upregulated by infection or autoimmune disease [21–23]. Therefore, in disorders with cellular infiltration such as inflammation (especially encephalitis) or cancer cell invasion, *B2M* expression levels may be significantly varied compared with normal tissue.

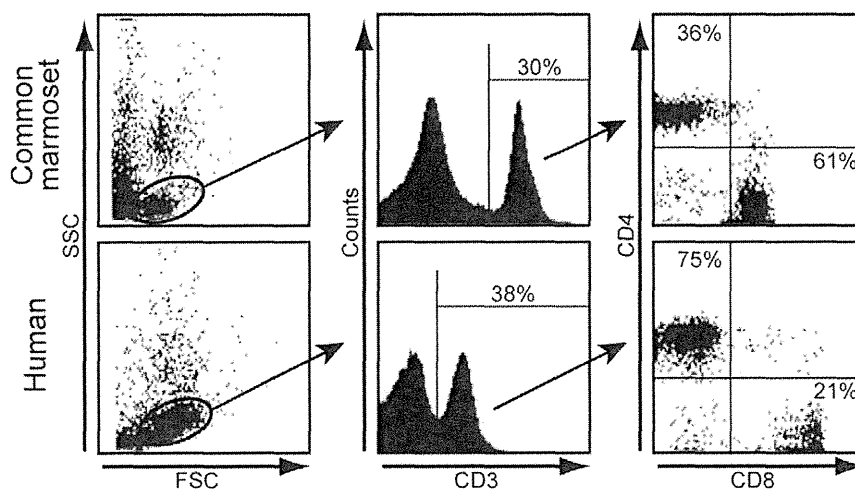


Figure 6. The ratio of CD4⁺ to CD8⁺ cells in common marmoset and human peripheral blood mononuclear cells (PBMCs) by flow cytometry. Representative scattered plots of FSC and SSC are shown in the left panels. Middle panels represent a histogram of CD3 analyzed in the lymphocyte gate. Gated CD3⁺ cells were analyzed for CD4 and CD8 expression (right panels).

doi:10.1371/journal.pone.0056296.g006

Table 3. CD8/CD4 ratio in PBMCs from young and old marmosets.

Age	Sex	% positive		CD8/CD4 ratio
		CD8	CD4	
3 month*	male	58.3	38.4	1.52
1.5 year	female	60.7	36.1	1.68
1.5 year*	male	55.1	41.5	1.33
2.0 year	male	52.7	44.6	1.18
10 year*	female	58.6	37.8	1.55
Mean \pm sd		57.1 \pm 3.2	39.7 \pm 3.4	1.45 \pm 0.20

*Only FACS analysis, but not qPCR, was done with PBMCs from these three marmosets.

doi:10.1371/journal.pone.0056296.t003

Thus, we predict that *B2M* may be unsuitable as a reference gene in many cases.

We assessed gene expression stability using the *geNorm* applet. As shown in Figure 2, *geNorm* analysis indicated that all tested genes were stable in each tissue. However, there were some trends in the stability ranking (Figure 3). For example, *TBP* in intestine segments and *SDHA* in brain segments represented prominently high stabilities. *GAPDH*, *ACTB*, *SDHA* and *TBP* were generally ranked high followed by *UBC*. In contrast, the stability of *rRNA* was generally low. This suggests the amount of mRNA is not always proportional to that of total RNA as reported by other studies [24,25]. In addition, *HPRT*, *rRNA* and *B2M* varied widely among tissues and rarely ranked high.

We analyzed the expression levels of CD antigens and cytokines by qPCR to compare the characteristics of peripheral blood leukocytes between common marmosets and humans (Figure 4). We observed that the expression levels of CD4 and IL-4 were lower in common marmosets than in humans. In contrast, the expression levels of IL-10, IL-12 β and IFN- γ were higher in common marmosets. We calculated PCR efficiency of each primer set and found there was no great difference between primers for common marmosets and those for humans (Tables 1 and 2). Thus, the differences in the gene expression levels between common marmosets and humans are not attributable to the differences in PCR efficiency.

We also observed that the CD4:CD8 ratio and Th1/Th2 balance were inverted in common marmosets by qPCR analysis (Figure 5). In particular, we confirmed the inverted CD4:CD8 ratio by flow cytometric analysis (Figure 6 and Table 3). The inverted CD4:CD8 ratio was stable over age. Of interest, we noted that the Th1/Th2 balance is different between common marmosets and humans, although we can only speculate on the cause of the difference. First, intestinal parasite infections may affect the Th1/Th2 balance by regulating expression of genes encoding cytokines [26–28]. In particular, protozoan parasites are potent stimulators of IFN- γ expression and Th1 responses [29]. Moreover, humans living in poor hygienic conditions in develop-

ing countries had higher Th1 cytokine levels compared with people in developed countries [30]. Although the common marmosets used in this study were maintained in specific pathogen-free conditions, we cannot rule out that such infectious agents may be one of a number of factors responsible for the difference in Th1/Th2 balance.

A second possible reason may be a difference in the number of cells producing the respective cytokines. As shown in Figure 6, the ratio of CD4⁺ to CD8⁺ cells were markedly different in total leukocytes from common marmosets and humans. Since IL-4 is mainly produced by CD4⁺ T cells [31,32], its expression level may be influenced by the CD4:CD8 ratio. However, this is not true for all the cytokines tested. For example, the expression levels of IL-2, IL-5 and IL-13, largely produced by T cells, were not significantly different between common marmosets and humans. Therefore, we suggest that the CD4:CD8 ratio has little effect on Th1/Th2 balance. IL-10 is produced by T cells and monocytes [33] and IL-12 β is naturally produced by dendritic cells and macrophages [34,35]. However, we could not verify these cell numbers in the common marmoset. Further studies are required to determine whether the numbers of cytokine-producing cells influence the expression levels of IL-10 and IL-12 β .

Another possibility is genetic variation. Bostik et al., reported distinct sequence differences in the promoter region or the proximal region of cytokine genes including IL-4, IL-10, IL-12 β and TNF- γ among humans, macaque and mangabey monkeys, which affected regulation of cytokine synthesis [36]. Jeong et al., reported that the expression level of IL-4 was lower in monkeys (baboon and macaque) than in hominoids (human and chimpanzee) while the expression levels of IL-12 β and the IFN- γ were higher in monkeys [37]. It is likely that Th1 dominant expression is common to primates other than hominoids and the difference in Th1/Th2 balance may be caused by genetic differences between common marmosets and humans.

The use of common marmoset is growing in popularity as a non-human primate model in many fields including autoimmune disease and infectious disease. In this study, we presented data regarding gene expression stabilities of common marmoset housekeeping genes and differences in the Th1/Th2 balance between common marmosets and humans. This difference may affect host defense and/or disease susceptibility, which should be carefully considered in biomedical research using common marmoset as an experimental model. We believe our data will contribute to future investigations using common marmoset models of various diseases.

Acknowledgments

We would like to acknowledge the efforts of Yasushi Ami in animal experiments. We also thank Ms. Hiro Yamada for technical assistance.

Author Contributions

Conceived and designed the experiments: YF TM K. Kitaura TS YH IK RS. Performed the experiments: YF K. Kitaura KS SS TT YK ST HK. Analyzed the data: YF RS. Contributed reagents/materials/analysis tools: K. Kumagai KS. Wrote the paper: TM K. Kitaura TS YH IK RS.

References

- Klug S, Neubert R, Stahlmann R, Thiel R, Rytffel B, et al. (1994) Effects of recombinant human interleukin 6 (rhIL-6) in marmosets (*Callithrix jacchus*). 1. General toxicity and hematological changes. *Arch Toxicol* 68: 619–631.
- Zühlke U, Weinbauer G (2003) The common marmoset (*Callithrix jacchus*) as a model in toxicology. *Toxicol Pathol* 31 Suppl: 123–127.
- Yaguchi M, Tabuse M, Ohta S, Ohkusu-Tsukada K, Takeuchi T, et al. (2009) Transplantation of dendritic cells promotes functional recovery from spinal cord injury in common marmoset. *Neurosci Res* 65: 384–92.
- Ando K, Maeda J, Inaji M, Okauchi T, Obayashi S, et al. (2008) Neurobehavioral protection by single dose 1-deprenyl against MPTP-induced parkinsonism in common marmosets. *Psychopharmacology (Berl)* 195: 509–516.
- Genain CP, Lee-Parritz D, Nguyen MH, Massacesi L, Joshi N, et al. (1994) In healthy primates, circulating autoreactive T cells mediate autoimmune disease. *J Clin Invest* 94: 1339–1345.
- Genain CP, Hauser SL (1997) Creation of a model for multiple sclerosis in *Callithrix jacchus* marmosets. *J Mol Med* 75: 187–197.

7. Bright H, Carroll AR, Watts PA, Fenton RJ (2004) Development of a GB virus B marmoset model and its validation with a novel series of hepatitis C virus NS3 protease inhibitors. *J Virol* 78: 2062–2071.
8. Adams AP, Aronson JF, Tardif SD, Patterson JL, Brasky KM, et al. (2008) Common marmosets (*Callithrix jacchus*) as a nonhuman primate model to assess the virulence of eastern equine encephalitis virus strains. *J Virol* 82: 9035–9042.
9. Mansfield K (2003) Marmoset models commonly used in biomedical research. *Comp Med* 53: 383–392.
10. Abbott DH, Barnett DK, Colman RJ, Yamamoto ME, Schultz-Darken NJ (2003) Aspects of common marmoset basic biology and life history important for biomedical research. *Comp Med* 53: 339–350.
11. Quint DJ, Buckham SP, Bolton EJ, Solari R, Champion BR, et al. (1990) Immunoregulation in the common marmoset, *Callithrix jacchus*: functional properties of T and B lymphocytes and their response to human interleukins 2 and 4. *Immunology* 69: 616–621.
12. Fukuoka T, Sumida K, Yamada T, Higuchi C, Nakagaki K, et al. (2010) Gene expression profiles in the common marmoset brain determined using a newly developed common marmoset-specific DNA microarray. *Neurosci Res* 66: 62–85.
13. Bustin SA, Nolan T (2004) Pitfalls of quantitative real-time reverse-transcription polymerase chain reaction. *J Biomol Tech* 15: 155–166.
14. Bustin SA, Benes V, Garson JA, Hellemans J, Huggett J, et al. (2009) The MIQE guidelines: minimum information for publication of quantitative real-time PCR experiments. *Clin Chem* 55: 611–622.
15. Vandesompele J, De Preter K, Pattyn F, Poppe B, Van Roy N, et al. (2002) Accurate normalization of real-time quantitative RT-PCR data by geometric averaging of multiple internal control genes. *Genome Biol* 3: RESEARCH0034.
16. Kametani Y, Suzuki D, Kohu K, Satake M, Suemizu H, et al. (2009) Development of monoclonal antibodies for analyzing immune and hematopoietic systems of common marmoset. *Exp Hematol* 37: 1318–1329.
17. Wiborg O, Pedersen MS, Wind A, Berglund LE, Marcker KA, et al. (1985) The human ubiquitin multigene family: some genes contain multiple directly repeated ubiquitin coding sequences. *EMBO J* 4: 755–759.
18. Drezon JM, Babinet C, Morello D (1993) Transcriptional control of MHC class I and beta 2-microglobulin genes in vivo. *J Immunol* 150: 2805–2813.
19. Lampson LA (1995) Interpreting MHC class I expression and class I/class II reciprocity in the CNS: reconciling divergent findings. *Microsc Res Tech* 32: 267–285.
20. Daar AS, Fuggle SV, Fabre JW, Ting A, Morris PJ (1984) The detailed distribution of HLA-A, B, C antigens in normal human organs. *Transplantation* 38: 287–292.
21. Kimura T, Griffin DE (2000) The role of CD8(+) T cells and major histocompatibility complex class I expression in the central nervous system of mice infected with neurovirulent Sindbis virus. *J Virol* 74: 6117–6125.
22. Keskinen P, Ronni T, Matikainen S, Lehtonen A, Julkunen I (1997) Regulation of HLA class I and II expression by interferons and influenza A virus in human peripheral blood mononuclear cells. *Immunology* 91: 421–429.
23. Mátrai Z, Németh J, Miklós K, Szabó Z, Masszi T (2009) Serum beta2-microglobulin measured by immunonephelometry: expression patterns and reference intervals in healthy adults. *Clin Chem Lab Med* 47: 585–589.
24. Solanas M, Moral R, Escrich E (2001) Unsuitability of using ribosomal RNA as loading control for Northern blot analyses related to the imbalance between messenger and ribosomal RNA content in rat mammary tumors. *Anal Biochem* 288: 99–102.
25. Valente V, Teixeira SA, Neder L, Okamoto OK, Oba-Shinjo SM, et al. (2009) Selection of suitable housekeeping genes for expression analysis in glioblastoma using quantitative RT-PCR. *BMC Mol Biol* 10: 17.
26. Bentwich Z, Weisman Z, Moroz C, Bar-Yehuda S, Kalinkovich A (1996) Immune dysregulation in Ethiopian immigrants in Israel: relevance to helminth infections? *Clin Exp Immunol* 103: 239–243.
27. Sacks D, Sher A (2002) Evasion of innate immunity by parasitic protozoa. *Nat Immunol* 3: 1041–1047.
28. Sher A, Coffman RL (1992) Regulation of immunity to parasites by T cells and T cell-derived cytokines. *Annu Rev Immunol* 10: 385–409.
29. Denkers EY, Gazzinelli RT (1998) Regulation and function of T-cell-mediated immunity during *Toxoplasma gondii* infection. *Clin Microbiol Rev* 11: 569–588.
30. Malhotra I, Ouma J, Wamachi A, Kioko J, Mungai P, et al. (1997) In utero exposure to helminth and mycobacterial antigens generates cytokine responses similar to that observed in adults. *J Clin Invest* 99: 1759–1766.
31. Abbas AK, Murphy KM, Sher A (1996) Functional diversity of helper T lymphocytes. *Nature* 383: 787–793.
32. Mosmann TR, Sad S (1996) The expanding universe of T-cell subsets: Th1, Th2 and more. *Immunol Today* 17: 138–146.
33. de Waal Malefyt R, Abrams J, Bennett B, Figdor CG, de Vries JE (1991) Interleukin 10(IL-10) inhibits cytokine synthesis by human monocytes: an autoregulatory role of IL-10 produced by monocytes. *J Exp Med* 174: 1209–1220.
34. Hsieh CS, Macatonia SE, Tripp CS, Wolf SF, O'Garra A, et al. (1993) Development of TH1 CD4+ T cells through IL-12 produced by Listeria-induced macrophages. *Science* 260: 547–549.
35. Macatonia SE, Hosken NA, Litton M, Vieira P, Hsieh CS, et al. (1995) Dendritic cells produce IL-12 and direct the development of Th1 cells from naive CD4+ T cells. *J Immunol* 154: 5071–5079.
36. Bostik P, Watkins M, Villinger F, Ansari AA (2004) Genetic analysis of cytokine promoters in nonhuman primates: implications for Th1/Th2 profile characteristics and SIV disease pathogenesis. *Clin Dev Immunol* 11: 35–44.
37. Jeong AR, Nakamura S, Mitsunaga F (2008) Gene expression profile of Th1 and Th2 cytokines and their receptors in human and nonhuman primates. *J Med Primatol* 37: 290–296.

Pathophysiologic Role of Histamine: Evidence Clarified by Histidine Decarboxylase Gene Knockout Mice

Hiroshi Ohtsu

Department of Applied Quantum Medical Engineering, School of Engineering, Tohoku University, Sendai, Japan

Key Words

Histamine function · L-Histidine decarboxylase gene knockout mice · Wound healing

Abstract

The role of histamine in various murine disease models has been clarified using histidine decarboxylase gene knockout mice. The mice were generated using conventional gene-targeting methods. Studies, including ours, using knockout mice have shown that the activity of histamine is not limited to allergic, peptic and neurologic functions as in the old paradigm, but extends to other processes related to wound healing, circulatory disease, immunology, oncology and infectious disease. The recent observation of the activity of newly cloned histamine receptors and a pathophysiologic effect of histamine has dramatically expanded our understanding of the scope of histamine function.

Copyright © 2012 S. Karger AG, Basel

L-Histidine Decarboxylase Gene Knockout Mice

L-Histidine decarboxylase gene knockout (HDC-KO) mice lack the ability to synthesize histamine and therefore histamine-dependent activation via any of the 4

known histamine receptors cannot occur in these animals [1]. These mice have been used to clarify the role of histamine in various conditions including anaphylactic responses and allergic inflammation [2–4], several neurophysiologic functions [5, 6], gastroenterologic disease [7–10] and cardiovascular disease [11]. Because it is difficult to achieve complete and long-lasting elimination of the effects of histamine in vivo using pharmacological approaches, HDC-KO mice are an excellent tool for studying the effect of chronic deprivation of histamine in disease models.

Histamine in Allergic Bronchial Asthma

Histamine is a major mediator that elicits a number of acute pathological responses in allergic bronchial asthma [12, 13]. The evidence supporting a pathophysiological role of histamine in the asthmatic state includes the release of histamine from cells participating in allergic responses, the replication of features of allergic inflammation by application of histamine, the reduction of allergic inflammation by histamine receptor antagonists and the reduced eosinophilia in mice genetically modified to not synthesize histamine [3]. Mast cells and basophils are considered to be major cell sources of histamine in aller-

gic reactions. Histamine release from these cells is triggered by the interaction of an allergen with specific immunoglobulin E (IgE) bound to the high-affinity IgE receptor on the cell membrane or by nonspecific stimuli including exercise or cold dry air. The actions of histamine in allergic asthma may be rather complicated since it not only has direct actions on smooth muscle and capillaries, but also indirect activity on immune cells and changes the immunological reaction or effect to sympathetic nerves, which leads to a change in the tone of bronchial smooth muscles.

The role of histamine in immunology has been a major topic of study over the past 10 years. Dendritic cells express H₁, H₂ and H₄ receptors [14], and their exposure to histamine induces a shift toward the dendritic type 2 cells that promote T helper 2 cell (Th2) immune responses [15, 16]. Studies with mice bearing a targeted deletion of the H₁ receptor (H₁R) show a reduced production of interferon gamma (IFN- γ) and increased interleukin (IL)-4 and IL-13 production (results that are more consistent with the Th1-polarizing function of this receptor [17]), and these mice are reported to be less sensitive to methacholine challenge [18]. However, the effect of an H₁R blocker in clinical asthma is controversial. Blockade of the H₄R on dendritic cells leads to decreases in cytokine and chemokine production and limits their ability to induce Th2 responses in T cells [19]. Recently, it was reported that H₄R blockade diminished airway hyperreactivity in a murine asthma model [20]. Therefore, the H₄R may potentially be useful as a therapeutic target in bronchial asthma.

We previously examined the role of endogenous histamine on eosinophilic recruitment and hyperresponsiveness in an allergic bronchial asthma mouse model using HDC-KO mice [3]. Histamine levels in the airways of HDC-KO mice were markedly diminished compared to wild-type mice [3]. Inhalation challenge with ovalbumin (OVA) in OVA-sensitized wild-type mice caused eosinophil accumulation in the lungs and airway hyperreactivity to methacholine. On the other hand, eosinophil recruitment to the lungs was significantly reduced in HDC-KO mice. Proliferation of eosinophils in the bone marrow was induced after OVA challenge in wild-type mice; however, this proliferation was significantly lower in HDC-KO mice. In contrast, airway hyperreactivity was not suppressed in HDC-KO mice. These results suggest that endogenous histamine is involved in the accumulation of eosinophils in the airways after allergic challenge, possibly via effects on the bone marrow proliferation. Since histamine has eosinophil

chemotactic activity via the H₄R [21], reduced eosinophilia in HDC-KO mice could be explained through activity at the H₄R. Allergen-induced airway hyperreactivity appeared to be independent of airway eosinophilia in this bronchial asthma model.

Histamine in a Systemic Anaphylaxis Model

Compared with other allergic disorders, such as asthma, allergic dermatitis and allergic rhinitis, the pathophysiology of anaphylaxis appears to be relatively simple. Antigens bind to IgE receptor molecules on inflammatory cells, activating the cells through the receptors and causing them to release mediators that increase vascular permeability and cause smooth muscle contractions, ultimately leading to urticaria, hypotension, dyspnea, abdominal cramping and diarrhea [22]. A systemic anaphylaxis reaction associated with human allergy can be elicited in mice that are passively sensitized with trinitrophenyl (TNP)-specific antibody and challenged with TNP₄-OVA as an allergen. The systemic anaphylactic reaction manifests as hypotension, airway obstruction and hypothermia [4]. The Fc ϵ receptor is expressed on the plasma membrane of mast cells and is bound to IgE antibodies. Antigen binding to IgE molecules leads to secretion of the granular content into the environmental fluid, and the secreted granular content triggers the symptoms observed in systemic anaphylaxis. The reaction starts from a few minutes after the allergen challenge, and comprises an increase in vascular permeability, contraction of smooth muscle and an increase in mucin secretion. Circulatory collapse is observed as hypotension, increased heart rate and decreased peripheral resistance, and eventually leads to death. To elucidate the role of histamine in each of these symptoms, we induced a passive systemic anaphylaxis reaction in HDC-KO mice and wild-type mice and compared the changes in these parameters [4]. Blood pressure dropped in both HDC-KO and wild-type mice. On the other hand, decreases in respiratory frequency and body temperature and elongation of expiratory duration occurred only in wild-type mice. Therefore, in this model, respiratory frequency, expiratory time and body temperature were shown to be controlled by the activity of histamine, but its contribution to blood pressure appeared to be minor. Since mast cell-deficient *Kit^W/Kit^{W-v}* mice did not show any decrease in body temperature compared to control mice, it was most plausible that histamine derived from mast cells contributed to the decrease in body temperature.

Histamine in Chronic Allergic Contact Dermatitis

Repeated application of 2,4,6-trinitrochlorobenzene (TNCB) produces chronic allergic contact dermatitis in the skin [23, 24]. We worked to observe the effect of histamine in this model [25]. In this experiment, acute contact dermatitis was induced on the seventh day after sensitization by painting on a single epicutaneous application of TNCB. Chronic contact dermatitis was provoked after repeated epicutaneous application of the same antigen. By using the combination of HDC-KO mice with the H₄R agonist, 4-methylhistamine, and wild-type mice with the H₄R antagonist, JNJ7777120, the activity mediated via the H₄R in this model was further analyzed *in vivo*. In this model, mast cells and eosinophils migrated to the subdermal chronic contact dermatitis lesion. The levels of Th1 and Th2 cytokines in the skin tissue and the serum IgE level were elevated. The recruitment of mast cells and eosinophils, and the increases in Th2 cytokine and serum IgE levels were at least partially effected through H₄R [25]. On the contrary, the elevation in Th1 cytokine level was suppressed by the activation of H₄R [25]. H₄R antagonists have been proposed as a treatment for allergic disease [26]. In our experiment, an H₄R antagonist appears to be a promising agent for the treatment of chronic contact dermatitis as well. We are now assessing the combined application of H₁ and H₄R antagonists and have observed an additive effect of this combination for the treatment of this skin model (unpubl. observation).

Histamine in Atherosclerosis

HDC mRNA levels in the human aorta increase during the progression of atherosclerosis. HDC protein has been localized to macrophage-derived foam cells and mononuclear cells including lymphocytes [27]. The effect of histamine on the sclerotic change depends on the vessel size and its localization. At the capillary level, histamine distends the vessel wall and exerts extravasation of blood. In contrast, at the muscular artery level, which includes coronary and mesenteric arteries, arteries are constricted by histamine, due to the contraction of medial smooth muscle cells. Histamine also has a proliferative effect on smooth muscle cells [28]. To clarify the role of histamine-producing cells and its effect in atherosclerosis, HDC expression in atherosclerotic arteries was observed after mice had received a bone marrow transfusion from green fluorescent protein (GFP)-transgen-

ic mice [11]. Two different atherosclerosis models were used – a ligation-induced and a cuff-induced vascular injury model. In the ligation model, the neointima of atherosclerotic carotid arteries contained HDC-positive cells expressing macrophage marker or smooth muscle antigens. Interestingly, after the bone marrow transfusion, GFP-positive cells were colocalized with the cells expressing macrophage and smooth muscle cell markers at early and intermediate stages in the ligation model. In contrast, in the cuff model, the HDC-positive cells, which were positive for Mac-3, were mainly located in the adventitia, as were the GFP-positive cells after the bone marrow transfusion. Therefore, in both models bone marrow-derived cells were recruited to the vessels and colocalized with HDC-positive cells. In comparison to wild-type mice, HDC-KO mice showed reduced neointimal thickening and a decreased intima-to-media ratio after inducing atherosclerotic lesions. These results indicate that the histamine produced from bone marrow-derived progenitor cells, which could transdifferentiate into smooth muscle cells or macrophage-like cells, is important for the formation of neointima and atheromatous plaques. Since apolipoprotein E (apoE) is reported to be an important regulator for atherosclerosis, we used apoE-KO mice to produce a diet-induced model of atherosclerosis. Interestingly again, HDC-KO mice, once crossed with apoE-KO mice, had a reduced extent of atherosclerosis. However, the cholesterol level in the double-gene KO mice was greater than in apoE-KO mice [29]. Since it was reported that vascular permeability to low-density lipoproteins was reduced in H₁R-KO mice, and low-density lipoproteins in the aortic wall appeared to be an important trigger of atherosclerosis [30], in apoE-and-HDC-double-KO mice, transport of serum cholesterol into the aortic wall may be suppressed and, as a result, it may accumulate intravenously.

Histamine and Immunity

Histamine is well known for its role in immune reactions and exerts its effects through histamine H₁–H₄ receptors [31]. Lately, the role of the H₄R in immune reactions is being investigated energetically [32]. Through H₄R, histamine functions not only in adaptive immune responses but also in innate immunity, *i.e.* through natural-killer (NK) cell chemotaxis [33] and cytokine release from invariant NK T cells (iNKT) [34]. In [34], HDC-KO mice had a numerical and functional deficit in iNKT cells as evidenced by a drastic decrease in IL-4 and IFN- γ pro-

duction by these cells after the injection of α -GalCer, a glycolipid widely used as a specific activator of iNKT cells. This deficiency of cytokine production was clarified by measuring cytokine levels in the serum and in the gated iNKT cells of HDC-KO mice. The defect was due to the lack of histamine since a single injection of histamine into HDC-KO mice sufficed to restore normal IL-4 and IFN- γ production. Histamine-induced functional recovery was shown to be mediated mainly through the H₄R since it could be prevented by a selective H₄R antagonist and by the demonstration of a similar iNKT cell deficit in H₄R-deficient (H₄R-KO) mice. These findings identify a novel function of histamine through the H₄R in modulating iNKT cell functions and demonstrate that it may contribute the initial host defense mechanism. Furthermore, since the production of IL-4 is important for antibody class-switching to produce IgE, it is possible that histamine is not only a canonical allergic effector molecule, but can also regulate the afferent phase of the allergic state as well.

Histamine in Wound Healing

The absence of histamine in HDC-KO mice resulted in delayed cutaneous wound healing and exogenously administered histamine was able to restore this response [35]. Furthermore, overproduction of histamine in HDC gene-transgenic mice accelerates the healing process compared with wild-type mice. These results indicate

that histamine accelerates cutaneous wound healing. In this case, mast cells are presumably the source of histamine, since mast cell-deficient *Kit^W/Kit^{W-v}* mice showed impaired wound healing, and the H₁R seemed to be important for the wound healing process, since an H₁R antagonist appeared to reduce the wound closure [36]. Macrophage recruitment and angiogenesis at the wound edge were specifically impaired in HDC-KO mice, and histamine supplementation reversed this response [35]. The protein level of basic fibroblast growth factor (bFGF) at the wound edge was higher in wild-type mice than in HDC-KO mice. SU5402, a specific antagonist to fibroblast growth factor receptor 1 (FGFR1) tyrosine kinase, applied topically to the wound surface, suppressed wound healing in wild-type mice, but not in HDC-KO mice. From these observations, the accelerated wound healing activity of histamine appeared to be mediated by the activity of bFGF. Recently, modulation of FGFR1a signaling in zebrafish was reported to reveal a genetic basis for the aggression-boldness syndrome through the activity of histamine [37]. This activity and the activity of histamine in wound healing being transmitted to FGF might constitute a feedback mechanism. The mechanism is awaiting clarification.

Disclosure Statement

The author declares that no financial or other conflict of interest exists in relation to the content of the article.

References

- Ohtsu H, Tanaka S, Terui T, Hori Y, Makabe-Kobayashi Y, Pejler G, Tchougounova E, Hellman L, Gertsenstein M, Hirasawa N, Sakurai E, Buzas E, Kovacs P, Csaba G, Kittel A, Okada M, Hara M, Mar L, Numayama-Tsuruta K, Ishigaki-Suzuki S, Ohuchi K, Ichikawa A, Falus A, Watanabe T, Nagy A: Mice lacking histidine decarboxylase exhibit abnormal mast cells. *FEBS Lett* 2001;502: 53–56.
- Hirasawa N, Ohtsu H, Watanabe T, Ohuchi K: Enhancement of neutrophil infiltration in histidine decarboxylase-deficient mice. *Immunology* 2002;107:217–221.
- Koarai A, Ichinose M, Ishigaki-Suzuki S, Yamagata S, Sugiura H, Sakurai E, Makabe-Kobayashi Y, Kuramasu A, Watanabe T, Shirato K, Hattori T, Ohtsu H: Disruption of L-histidine decarboxylase reduces airway eosinophilia but not hyperresponsiveness. *Am J Respir Crit Care Med* 2003;167:758–763.
- Makabe-Kobayashi Y, Hori Y, Adachi T, Ishigaki-Suzuki S, Kikuchi Y, Kagaya Y, Shirato K, Nagy A, Ujike A, Takai T, Watanabe T, Ohtsu H: The control effect of histamine on body temperature and respiratory function in IgE-dependent systemic anaphylaxis. *J Allergy Clin Immunol* 2002;110:298–303.
- Parmentier R, Ohtsu H, Djebbara-Hannas Z, Valatx JL, Watanabe T, Lin JS: Anatomical, physiological, and pharmacological characteristics of histidine decarboxylase knockout mice: evidence for the role of brain histamine in behavioral and sleep-wake control. *J Neurosci* 2002;22:7695–7711.
- Dere E, De Souza-Silva MA, Spieler RE, Lin JS, Ohtsu H, Haas HL, Huston JP: Changes in motoric, exploratory and emotional behaviours and neuronal acetylcholine content and 5-HT turnover in histidine decarboxylase-KO mice. *Eur J Neurosci* 2004;20:1051–1058.
- Andou A, Hisamatsu T, Okamoto S, Chinen H, Kamada N, Kobayashi T, Hashimoto M, Okutsu T, Shimbo K, Takeda T, Matsumoto H, Sato A, Ohtsu H, Suzuki M, Hibi T: Dietary histidine ameliorates murine colitis by inhibition of proinflammatory cytokine production from macrophages. *Gastroenterology* 2009;136:564–574.
- Tanaka S, Hamada K, Yamada N, Sugita Y, Tonai S, Hunyady B, Palkovits M, Falus A, Watanabe T, Okabe S, Ohtsu H, Ichikawa A, Nagy A: Gastric acid secretion in L-histidine decarboxylase-deficient mice. *Gastroenterology* 2002;122:145–155.
- Nakamura E, Kataoka T, Furutani K, Jimbo K, Aihara T, Tanaka S, Ichikawa A, Ohtsu H, Okabe S: Lack of histamine alters gastric mucosal morphology: comparison of histidine decarboxylase-deficient and mast cell-deficient mice. *Am J Physiol Gastrointest Liver Physiol* 2004;287:G1053–G1061.

- 10 Yokoyama M, Yokoyama A, Mori S, Takahashi HK, Yoshino T, Watanabe T, Ohtsu H, Nishibori M: Inducible histamine protects mice from *P. acnes*-primed and LPS-induced hepatitis through H2-receptor stimulation. *Gastroenterology* 2004;127:892–902.
- 11 Sasaguri Y, Wang KY, Tanimoto A, Tsutsui M, Ueno H, Murata Y, Kohno Y, Yamada S, Ohtsu H: Role of histamine produced by bone marrow-derived vascular cells in pathogenesis of atherosclerosis. *Circ Res* 2005;96:974–981.
- 12 Dunford PJ, Holgate ST: The role of histamine in asthma. *Adv Exp Med Biol* 2011;709:53–66.
- 13 White MV: The role of histamine in allergic diseases. *J Allergy Clin Immunol* 1990;86:599–605.
- 14 Gutzmer R, Langer K, Lisewski M, Mommert S, Rieckborn D, Kapp A, Werfel T: Expression and function of histamine receptors 1 and 2 on human monocyte-derived dendritic cells. *J Allergy Clin Immunol* 2002;109:524–531.
- 15 Caron G, Delneste Y, Roelandts E, Duez C, Bonnefoy JY, Pestel J, Jeannin P: Histamine polarizes human dendritic cells into Th2 cell-promoting effector dendritic cells. *J Immunol* 2001;167:3682–3686.
- 16 Mazzoni A, Young HA, Spitzer JH, Visintin A, Segal DM: Histamine regulates cytokine production in maturing dendritic cells, resulting in altered T cell polarization. *J Clin Invest* 2001;108:1865–1873.
- 17 Jutel M, Watanabe T, Klunker S, Akdis M, Thomet OA, Malolepszy J, Zak-Nejmark T, Koga R, Kobayashi T, Blaser K, Akdis CA: Histamine regulates T-cell and antibody responses by differential expression of H1 and H2 receptors. *Nature* 2001;413:420–425.
- 18 Bryce PJ, Mathias CB, Harrison KL, Watanabe T, Geha RS, Oettgen HC: The H1 histamine receptor regulates allergic lung responses. *J Clin Invest* 2006;116:1624–1632.
- 19 Dunford PJ, O'Donnell N, Riley JP, Williams KN, Karlsson L, Thurmond RL: The histamine H4 receptor mediates allergic airway inflammation by regulating the activation of CD4+ T cells. *J Immunol* 2006;176:7062–7070.
- 20 Cowden JM, Riley JP, Ma JY, Thurmond RL, Dunford PJ: Histamine H4 receptor antagonism diminishes existing airway inflammation and dysfunction via modulation of Th2 cytokines. *Resp Res* 2010;11:86.
- 21 O'Reilly M, Alpert R, Jenkinson S, Gladue RP, Foo S, Trim S, Peter B, Trevethick M, Fiddock M: Identification of a histamine H4 receptor on human eosinophils – role in eosinophil chemotaxis. *J Recept Signal Transduct Res* 2002;22:431–448.
- 22 MacGlashan Jr MD: Biochemical events in basophil/mast cell activation and mediator release; in Adkinson NF Jr et al (eds): *Middleton's Allergy*. Philadelphia, Mosby, 2009, pp 235–258.
- 23 Kitagaki H, Fujisawa S, Watanabe K, Hayakawa K, Shiohara T: Immediate-type hypersensitivity response followed by a late reaction is induced by repeated epicutaneous application of contact sensitizing agents in mice. *J Invest Dermatol* 1995;105:749–755.
- 24 Kitagaki H, Ono N, Hayakawa K, Kitazawa T, Watanabe K, Shiohara T: Repeated elicitation of contact hypersensitivity induces a shift in cutaneous cytokine milieu from a T helper cell type 1 to a T helper cell type 2 profile. *J Immunol* 1997;159:2484–2491.
- 25 Seike M, Furuya K, Omura M, Hamada-Watanabe K, Matsushita A, Ohtsu H: Histamine H(4) receptor antagonist ameliorates chronic allergic contact dermatitis induced by repeated challenge. *Allergy* 2010;65:319–326.
- 26 Thurmond RL, Gelfand EW, Dunford PJ: The role of histamine H1 and H4 receptors in allergic inflammation: the search for new antihistamines. *Nature Rev Drug Discov* 2008;7:41–53.
- 27 Higuchi S, Tanimoto A, Arima N, Xu H, Murata Y, Hamada T, Makishima K, Sasaguri Y: Effects of histamine and interleukin-4 synthesized in arterial intima on phagocytosis by monocytes/macrophages in relation to atherosclerosis. *FEBS Lett* 2001;505:217–222.
- 28 Miyazawa N, Watanabe S, Matsuda A, Kondo K, Hashimoto H, Umemura K, Nakashima M: Role of histamine H1 and H2 receptor antagonists in the prevention of intimal thickening. *Eur J Pharmacol* 1998;362:53–59.
- 29 Wang KY, Tanimoto A, Guo X, Yamada S, Shimajiri S, Murata Y, Ding Y, Tsutsui M, Kato S, Watanabe T, Ohtsu H, Hirano K, Kohno K, Sasaguri Y: Histamine deficiency decreases atherosclerosis and inflammatory response in apolipoprotein E knockout mice independently of serum cholesterol level. *Arterioscler Thromb Vasc Biol* 2011;31:800–807.
- 30 Rozenberg I, Sluka SH, Rohrer L, Hofmann J, Becher B, Akhmedov A, Soliz J, Mocharla P, Boren J, Johansen P, Steffel J, Watanabe T, Luscher TF, Tanner FC: Histamine H1 receptor promotes atherosclerotic lesion formation by increasing vascular permeability for low-density lipoproteins. *Arterioscler Thromb Vasc Biol* 2010;30:923–930.
- 31 Akdis CA, Simons FE: Histamine receptors are hot in immunopharmacology. *Eur J Pharmacol* 2006;533:69–76.
- 32 Zhang M, Thurmond RL, Dunford PJ: The histamine H(4) receptor: a novel modulator of inflammatory and immune disorders. *Pharmacol Therapeut* 2007;113:594–606.
- 33 Damaj BB, Becerra CB, Esber HJ, Wen Y, Maghazachi AA: Functional expression of H4 histamine receptor in human natural killer cells, monocytes, and dendritic cells. *J Immunol* 2007;179:7907–7915.
- 34 Leite-de-Moraes MC, Diem S, Michel ML, Ohtsu H, Thurmond RL, Schneider E, Dy M: Cutting edge: Histamine receptor H4 activation positively regulates in vivo il-4 and IFN-gamma production by invariant NKT cells. *J Immunol* 2009;182:1233–1236.
- 35 Numata Y, Terui T, Okuyama R, Hirasawa N, Sugiura Y, Miyoshi I, Watanabe T, Kuramasu A, Tagami H, Ohtsu H: The accelerating effect of histamine on the cutaneous wound-healing process through the action of basic fibroblast growth factor. *J Invest Dermatol* 2006;126:1403–1409.
- 36 Weller K, Foitzik K, Paus R, Syska W, Maurer M: Mast cells are required for normal healing of skin wounds in mice. *FASEB J* 2006;20:2366–2368.
- 37 Norton WH, Stumpfenhorst K, Faus-Kessler T, Folchert A, Rohner N, Harris MP, Callebort J, Bally-Cuif L: Modulation of FGFR1a signaling in zebrafish reveals a genetic basis for the aggression-boldness syndrome. *J Neurosci* 2011;31:13796–13807.

The antagonism of histamine H1 and H4 receptors ameliorates chronic allergic dermatitis via anti-pruritic and anti-inflammatory effects in NC/Nga mice

Y. Ohsawa & N. Hirasawa

Laboratory of Pharmacotherapy of Life-Style Related Diseases, Graduate School of Pharmaceutical Sciences, Tohoku University, Sendai, Japan

To cite this article: Ohsawa Y, Hirasawa N. The antagonism of histamine H1 and H4 receptors ameliorates chronic allergic dermatitis via anti-pruritic and anti-inflammatory effects in NC/Nga mice. *Allergy* 2012; **67**: 1014–1022.

Keywords

atopic dermatitis; histamine H1 receptor; histamine H4 receptor; keratinocytes; mast cells.

Correspondence

Yusuke Ohsawa, Laboratory of Pharmacotherapy of Life-Style Related Diseases, Graduate School of Pharmaceutical Sciences, Tohoku University, Sendai, Japan.
Tel.: +81-22-795-5915
Fax: +81-22-795-5504
E-mail: yuusuke_ohsawa@pharm.kissei.co.jp

Accepted for publication 01 May 2012

DOI:10.1111/j.1398-9995.2012.02854.x

Edited by: Angela Haczku

Abstract

Background: Although histamine H1 receptor (H1R) antagonists are commonly used to treat atopic dermatitis, the treatment is not always effective. The histamine H4 receptor (H4R) was recently described as important to the pruritus in dermatitis. Here, we investigated whether the combination of a H1R antagonist plus a H4R antagonist attenuates chronic dermatitis in NC/Nga mice.

Methods: Chronic dermatitis was developed by repeated challenges with picryl chloride on the dorsal back and ear lobes. The therapeutic effects of the H1R antagonist olopatadine and H4R antagonist JNJ7777120 on scratching and the severity of dermatitis were evaluated. In addition, the mechanisms responsible for the anti-allergic effects of H1R and/or H4R antagonism were examined using bone marrow-derived mast cells (BMMC) and keratinocytes.

Results: JNJ7777120 attenuated scratching behavior after a single administration and improved dermatitis, as assessed with clinical scores, pathology, and cytokine levels in skin lesions when administered repeatedly. These effects were augmented by combined treatment with olopatadine, having a similar therapeutic efficacy to prednisolone. JNJ7777120 inhibited dose-dependently the production of thymus and activation-regulated chemokine/CCL17 and macrophage-derived chemokine/CCL22 from antigen-stimulated BMMC. In addition, olopatadine reversed the histamine-induced reduction of semaphorin 3A mRNA in keratinocytes.

Conclusion: Combined treatment with H1R and H4R antagonists may have a significant therapeutic effect on chronic dermatitis through the synergistic inhibition of pruritus and skin inflammation.

Atopic dermatitis (AD) is an allergic inflammatory disease characterized by intense pruritus, chronic eczematous plaques, and relapsing inflammation induced by repeated exposure to an antigen. The inflamed skin contains mast cells, eosinophils, and Th2 cells and exhibits histological abnormalities such as scaling, crusting, and lichenoid papules

Abbreviations

AD, atopic dermatitis; BMMC, bone marrow-derived mast cells; H1R, histamine H1 receptor; H4R, histamine H4 receptor; HDC, histidine decarboxylase; MDC, macrophage-derived chemokine; NGF, nerve growth factor; PICl, picryl chloride; Sema3A, semaphorin 3A; TARC, thymus and activation-regulated chemokine; TSLP, thymic stromal lymphopoietin.

(1, 2). The cytokine milieu of the inflamed skin shows Th2-dominant responses indicated by production of IL-4, IL-5, and IL-13 (2). These responses are triggered by thymic stromal lymphopoietin (TSLP) produced by keratinocytes (3).

Vigorous pruritus is the most important issue for a therapeutic strategy in patients with AD, and the pruritus associated with AD is poorly controlled clinically and affects the quality of life of patients. Histamine has been extensively studied for its pruritogenic effects (4, 5). It has been shown to be a potent pruritogen when applied to both human normal skin (6) and diseased skin (7). However, there is no clear evidence that histamine H1 receptor (H1R) antagonists inhibit it.

Four types of histamine receptors have been identified to date. The fourth, the histamine H4 receptor (H4R), which

was cloned in 2000, is expressed on several hematopoietic cells and plays important roles in the activation of mast cells, eosinophils, monocytes, dendritic cells, and T cells (8–11). Thus, H4R is considered a new therapeutic target for allergic inflammation in case of AD, asthma, and rhinitis (12–15). Using H4R-deficient mice or a H4R antagonist, it has been indicated that H4R plays roles in pruritus and acute inflammation (12, 13, 16–19). Previously, we examined the inhibitory effects of anti-histamines, which include pyrillamine, an H1R antagonist, cimetidine, an H2R antagonist, and thio-peramide, an H3R/H4R antagonist on TPA-enhanced picryl chloride (PiCl)-induced allergic dermatitis in mice (12). As the results, we found that the H2R antagonist showed only a slight inhibition. In contrast, the H1R antagonist significantly inhibited the increase in the ear thickness in the early phase and the H3R/H4R antagonist significantly inhibited the delayed phase responses such as eosinophil infiltration, and the combination of the H1R antagonist and the H3R/H4R antagonist showed additive effects.

As far, there were several trials of the combination of H1R antagonist and H2R antagonist on AD, which indicated no benefit (20). Here, we investigated whether or not a H4R antagonist or H4R plus H1R antagonist inhibits chronic allergic dermatitis in NC/Nga mice. The mechanisms of anti-allergic function via the inhibition of H4R and/or H1R were also verified *in vitro*.

Materials and methods

Animals

Male NC/Nga mice (specific pathogen-free) aged 6 weeks were purchased from Japan SLC. All mice were treated in accordance with procedures approved by the local Animal Ethics Committee.

Sensitization and repeated challenge

For sensitization, 150 μ l of a 5% (w/v) picryl chloride (Nacalai tesque, Kyoto, Japan) solution (3 : 1 in acetone/ethanol) was applied using a micropipette to the thoracic and abdominal areas. Five days later, the first challenge was performed by applying 200 μ l of a 1.2% (w/v) PiCl solution in olive oil, to the back and to the left and right ears. This procedure was repeated once a week for up to 10 weeks.

Drugs

Olopatadine (3 mg/kg; AK scientific, Union, CA, USA), JNJ7777120 (30 mg/kg; provided by Johnson & Johnson Pharmaceutical Research & Development, L.L.C., San Diego, CA, USA), and prednisolone (3 mg/kg; Sigma-Aldrich, St. Louis, MO, USA) were suspended in 0.5% carboxyl methylcellulose and administered orally in a volume of 5 ml/kg every other day from 5 to 10 weeks after the sensitization. The doses of these histamine antagonists were selected according to the previous reports (16, 18, 21, 22). For *in vitro* experiments, histamine antagonists were dissolved in DMSO and the final concentration of DMSO was adjusted to 0.1–0.2%.

Real-time PCR for histidine decarboxylase (HDC) and measurement of plasma levels of histamine

Forty-eight hours after the fifth challenge at 5 weeks, blood and the ear lobes were collected. The level of histamine in plasma was determined using a Histamine EIA kit (SPI-Bio, Montigny le Bretonneux, France), and total RNA of the tissues was extracted using an RNeasy Fibrous Tissue Kit (Qiagen, Hilden, Germany). The primers for real-time PCR were (forward) 5'-TGTGTCCGTCGTGGATCTGA-3' and (Reverse) 5'-TTGCTGTTGAAGTCGCAGGAG-3' for mouse GAPDH, and (forward) 5'-TCCATTAAGCTGTGGTTTGTGATTC-3' and (reverse) 5'-CGCTTCTGACCAGAGATTCAAAGTA-3' for mouse HDC.

Counting of scratching and scoring of dermatitis

Three days after the fifth challenge, the number of times the mice scratched during 2 h after receiving a single drug dose was counted and then the severity of the dermatitis was evaluated once a week from week 5 to 10 following repeated treatment. The observation items were (I) flare and hemorrhage, (II) edema, (III) excoriation and erosion, and (IV) incrustation and xerosis. Evaluation items were scored as follows: 0 = no sign; 1 = mild; 2 = moderate; 3 = severe. The sum of the scores for each evaluation item (maximum score: 12) was taken as the dermatitis score.

Histological analysis

Ten weeks after the sensitization, the ear lobe was excised and paraffin-embedded sections were prepared. Serial sections were stained with hematoxylin–eosin or 0.05% toluidine blue. CD4⁺ helper T cells were immunostained with anti-mouse CD4 antibody (R&D systems, Minneapolis, MN, USA).

Measurement of levels of cytokines in skin lesions and IgE in plasma

Ten weeks after the sensitization, the ear lobe was immersed in liquid nitrogen, crushed with an SK Mill (Tokken, Kashiwa, Japan), and suspended in 1 ml of PBS containing a protease inhibitor (CompleteTM; Roche Diagnostics, Mannheim, Germany). The suspension was centrifuged at 1200 g for 10 min, and the supernatants of tissue homogenates and the plasma were used to analyze the levels of IL-4, IL-5, TSLP (Biolegend, San Diego, CA, USA), thymus and activation-regulated chemokine (TARC) (R&D systems), nerve growth factor (NGF) (Promega, Madison, WI, USA), and plasma IgE (Biolegend) with ELISA kits.

Preparation of bone marrow-derived mast cells

Bone marrow-derived mast cells (BMMC) were prepared from the bone marrow cells aspirated from NC/Nga mice (6–8 weeks old). The bone marrow cells were cultured in RPMI1640 medium that contained 10% FBS, HEPES (25 mM), penicillin (100 units/ml), streptomycin (100 μ g/ml),

and recombinant mIL-3 (300 pg/ml; R&D systems) for 9 days. More than 80% of bone marrow cells were positive for FcεRI and c-kit, as assessed by flow cytometric analysis with PE-labeled anti-mouse FcεRI antibody (Biolegend) and FITC-labeled anti-mouse c-kit antibody (Biolegend).

Stimulation of BMMC with anti-DNP IgE and DNP-BSA, and measurement of levels of thymus and activation-regulated chemokine (TARC/CCL17) and macrophage-derived chemokine (MDC/CCL22)

Bone marrow-derived mast cells were primed overnight with anti-DNP IgE (0.5 µg/ml; Sigma-Aldrich). The cells were treated with olopatadine and/or JNJ7777120 for 30 min and then stimulated with DNP-BSA (1–25 ng/ml; LSL, Japan) for 24 h. The amount of histamine in the culture medium was determined by EIA, and TARC and MDC levels were measured with ELISA kits (R&D systems).

Change of semaphorin 3A (Sema3A) mRNA levels after histamine treatment in PAM212 cells

PAM 212, a murine keratinocyte cell line, kindly supplied by Dr. S. H. Yuspa, NCI, NIH, USA, was cultured in RPMI1640 medium containing 10% FBS, penicillin (100 units/ml), streptomycin (100 µg/ml), and HEPES (25 mM). The cells were incubated for 30 min in medium containing olopatadine and then stimulated with histamine at various concentrations. The level of mRNA for Sema3A was evaluated by real-time PCR. The primers for PCR were (forward) 5'-AGATGCTCCATTCCAGTTTGTTTAC-3' and (Reverse) 5'-ACATAAGCCACCGCATCACTTGTA-3' for mouse Sema3A.

Statistical significance

Values are presented as the standard error of the mean. The statistical significance of the results was analyzed with the Student's *t*-test, Dunnett's test for parametric analysis, or corresponding to score for nonparametric analysis.

Results

Increased histamine production and release in mice with PiCl-induced chronic dermatitis

The NC/Nga mice treated with PiCl for 5 weeks developed moderate dermatitis with erythema, crusting and skin erosion on the treated skin and ear lobes (Fig. 1B) compared with intact mice (Fig. 1A). Forty-eight hours after the fifth treatment, the level of histamine in plasma (Fig. 1C) and the level of HDC mRNA in skin lesions (Fig. 1D) were significantly increased.

Effects of single administration of olopatadine and JNJ7777120 on scratching behavior

Three days after the fifth challenge, drugs were administered and scratching counts were determined. As shown in Fig. 1E,

the number of times the mice scratched during 2 h was significantly increased. Administration of olopatadine or JNJ7777120 apparently reduced the counts, and combined treatment significantly decreased them. The anti-pruritus effect of the combined treatment was as potent as that of prednisolone.

Amelioration of dermatitis by repeated administration of olopatadine and JNJ7777120

Olopatadine and/or JNJ7777120 were administered every other day after the fifth treatment with PiCl, and the dermatitis score was evaluated until week 10. The dermatitis score progressively increased dependent on the number of challenges with PiCl. JNJ7777120, but not olopatadine, prevented this increase (Fig. 1F). Interestingly, combined treatment had a significant effect from 8 weeks (Fig. 1F), and the severity of the dermatitis was reduced about 50% compared with the control group at 10 weeks. Consistent with the anti-pruritic effects, dual inhibition of H1R and H4R was as effective as prednisolone.

Effects of repeated administration of olopatadine and JNJ7777120 on histological changes and the number of mast cells

Histological examination revealed that the repeated treatment with PiCl caused severe acanthosis and the infiltration by inflammatory cells including lymphocytes and eosinophils of the ear lobe (Fig. 2B, E). The number of mast cells also increased significantly (Fig. 2G, I). Combined treatment with olopatadine and JNJ7777120 improved the hyperkeratosis (Fig. 2C, F). JNJ7777120 decreased the number of mast cells (Fig. 2H, I). Olopatadine alone did not decrease but augmented the inhibitory effects of JNJ7777120 (Fig. 2I).

Effects of repeated administration of olopatadine and JNJ7777120 on levels of cytokines in tissue and IgE in plasma

Next, we assessed the levels of IL-4, IL-5, TSLP, TARC, and NGF in tissue, and IgE in plasma at 10 weeks after the sensitization. Olopatadine decreased the level of NGF but not IL-4, IL-5, TSLP, TARC, or IgE (Fig. 3). In contrast, JNJ7777120 not only significantly decreased the NGF levels but also markedly inhibited the increases in IL-4, IL-5, TSLP, and TARC (Fig. 3). Although neither olopatadine nor JNJ7777120 alone reduced the plasma IgE level, in combination they inhibited the increase in IgE level similar to prednisolone (Fig. 3F). The production of MDC in tissue was not significantly inhibited by olopatadine, JNJ7777120, and prednisolone (data not shown).

Effects of olopatadine and JNJ7777120 on production of TARC and MDC in BMMC

To analyze the mechanism behind the anti-inflammatory effects of H1R and H4R antagonists, we tested whether olopatadine and/or JNJ7777120 inhibit TARC and MDC

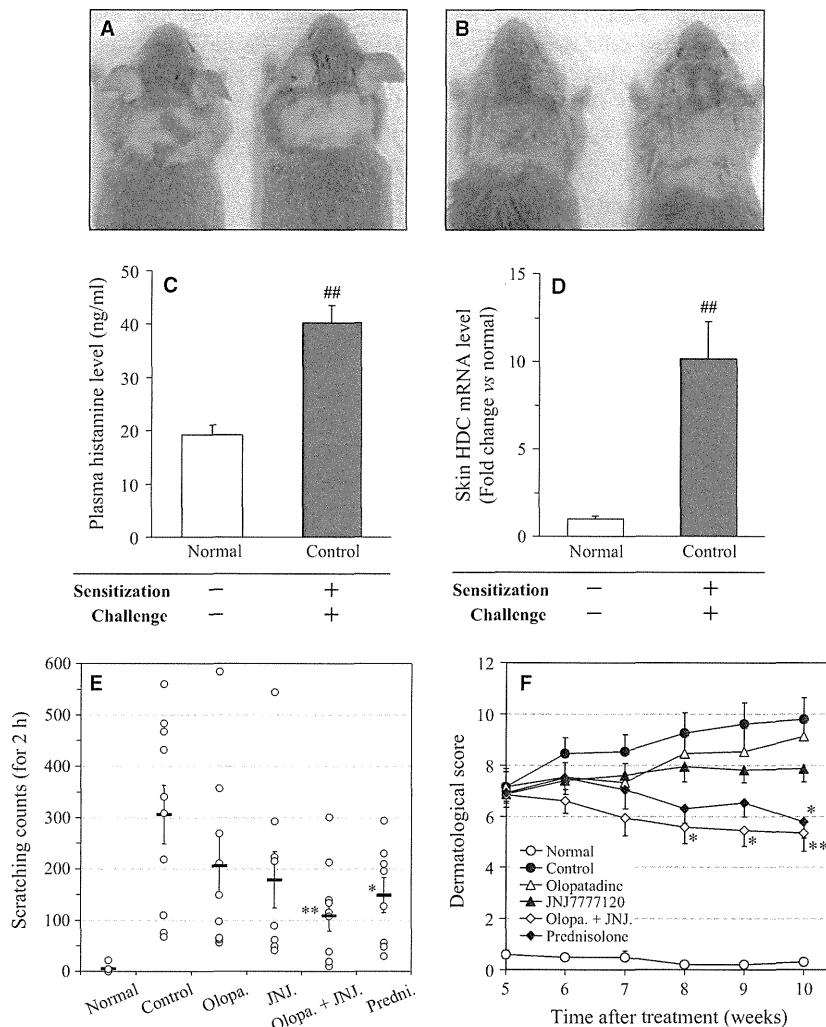


Figure 1 Increased histamine levels in picryl chloride (Picl)-induced chronic allergic dermatitis and effects of olopatadine and JNJ777120 on scratching counts and dermatological scores. NC/Nga mice were sensitized and challenged as described in 'Materials and Methods'. Forty-eight hours after the challenge, mice of the normal group (intact mice, A) and control group (Picl-sensitized and challenged mice, B) were photographed. The levels of histamine in plasma (C) and histidine decarboxylase (HDC) mRNA in the

produced by BMMC. Bone marrow cells prepared from NC/Nga mice were induced to differentiate into FcεRI⁺/c-kit⁺ mast cells (more than 80%) over 9 days (Fig. 4A). The stimulation of BMMC with the antigen increased the levels of histamine (Fig. 4B), TARC, and MDC (Fig. 4C) in the medium collected at 24 h. The histamine release was slightly inhibited by olopatadine at 10 μM (about 16% inhibition) but not JNJ777120 at 30 μM (data not shown). The production of TARC and MDC was inhibited slightly by olopatadine at 10 μM and significantly by JNJ777120 in a dose-dependent manner (30–100 μM) (Fig. 4C). The H3R/H4R antagonist thioperamide (100 μM) also suppressed the production of TARC (Fig. 4D). Furthermore, JNJ777120 plus olopatadine inhibited additively TARC production

inflamed skin (D) were determined. Three days after the fifth challenge, mice were orally administered olopatadine (3 mg/kg), JNJ777120 (30 mg/kg), olopatadine plus JNJ777120, or prednisolone (3 mg/kg), and then, scratching counts for 2 h were determined (E). The severity of the dermatitis was scored once a week from week 5 to 10 during repeated administration (F). Statistical significance; ##*P* < 0.01 vs normal group (*n* = 4), **P* < 0.05 and ***P* < 0.01 vs control group (*n* = 6–10).

(Fig. 4D). It was unlikely that JNJ777120 reduced the production of these cytokines via toxic effects because JNJ777120 did not reduce the antigen-induced release of IL-13 (data not shown).

Consistent with the reduction in TARC and MDC production in BMMC, the infiltration of CD4-positive cells in the skin 10 weeks after the sensitization was decreased by the combined treatment with olopatadine and JNJ777120 (Fig. 4E, F).

Effects of olopatadine on histamine-induced down-regulation of *Sema3A* expression in PAM212 cells

Finally, we tested whether olopatadine and/or JNJ777120 affect the level of mRNA for *Sema3A*, the regulatory

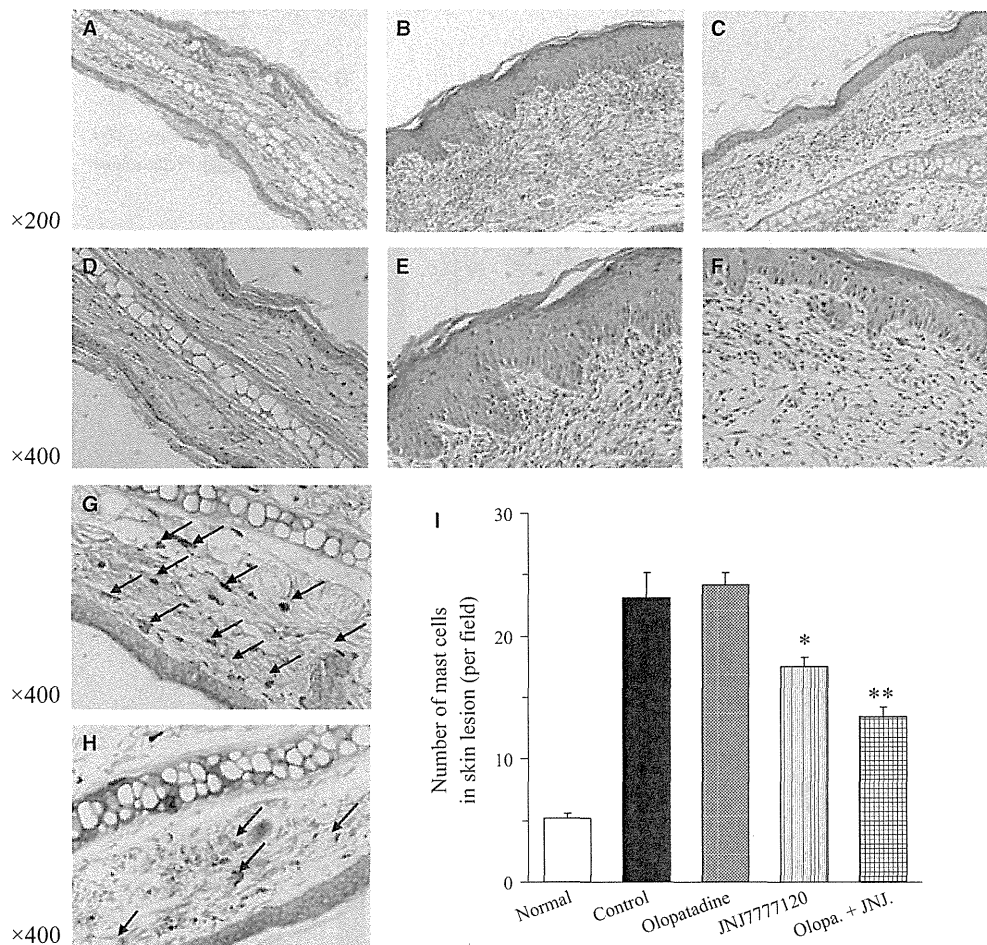


Figure 2 Effects of olopatadine and JNJ777120 on histological changes in mice treated repeatedly with picryl chloride (PiCl). Ten weeks after the sensitization, skin specimens prepared from intact mice (normal group; A, D), PiCl-treated mice (control group; B, E), and PiCl-treated mice administered olopatadine plus JNJ777120 (C, F) were stained with hematoxylin and eosin and observed with a light

microscope at magnification $\times 200$ (A, B, C) and $\times 400$ (D, E, F). The skin specimens prepared from PiCl-treated mice (G) and PiCl-treated mice administered olopatadine plus JNJ777120 (H) were stained with toluidine blue, and the numbers of mast cells were counted from four fields with a light microscope $\times 400$ (I). Statistical significance; * $P < 0.05$ and ** $P < 0.01$ vs control group ($n = 4-5$).

factor of neuronal elongation. The expression of H1R was detected by real-time PCR, but H4R was not detected in unstimulated and histamine-stimulated PAM212 cells (data not shown). The level of mRNA for Sema3A was decreased by histamine at $10 \mu\text{M}$ (Fig. 5A). The level reached a minimum at 3 h and slowly recovered over the next 9 h (Fig. 5B). The histamine-induced reduction in the level of Sema3A mRNA was antagonized by olopatadine (Fig. 5C) but not by JNJ777120 at $30 \mu\text{M}$ (data not shown).

Discussion

In this study, we demonstrated that the H1R antagonist olopatadine and H4R antagonist JNJ777120 improved scratching behavior and skin inflammation in a model of chronic allergic dermatitis established in NC/Nga mice. The effectiveness of the combined treatment against the dermatitis was almost equal to that of prednisolone.

Skin aberrations such as erythema, lichenification, and erosion accompanied the scratching behavior. The findings that histamine level in plasma and mRNA level for HDC in skin tissue were elevated in mice with chronic inflammation suggested histamine to be involved in the development of chronic allergic dermatitis in this model. As plasma histamine levels were reported to be significantly higher in patients with AD than controls (23, 24), this NC/Nga-based model of chronic dermatitis is an important tool for studying the roles of histamine in AD.

Recently, the anti-allergic effects of H4R antagonists were mainly evaluated in dermatitis model in mice (13, 17–19). Rossbach et al. (17) reported that a combination of H4R and H1R antagonism has prophylactic effects on acute hapten-induced scratching, but not chronic dermatitis. Only the study by Suwa et al. (19) was evaluated therapeutic effects for a H4R antagonist, but is not evaluated about benefits on combined treatment of a H1R and a H4R

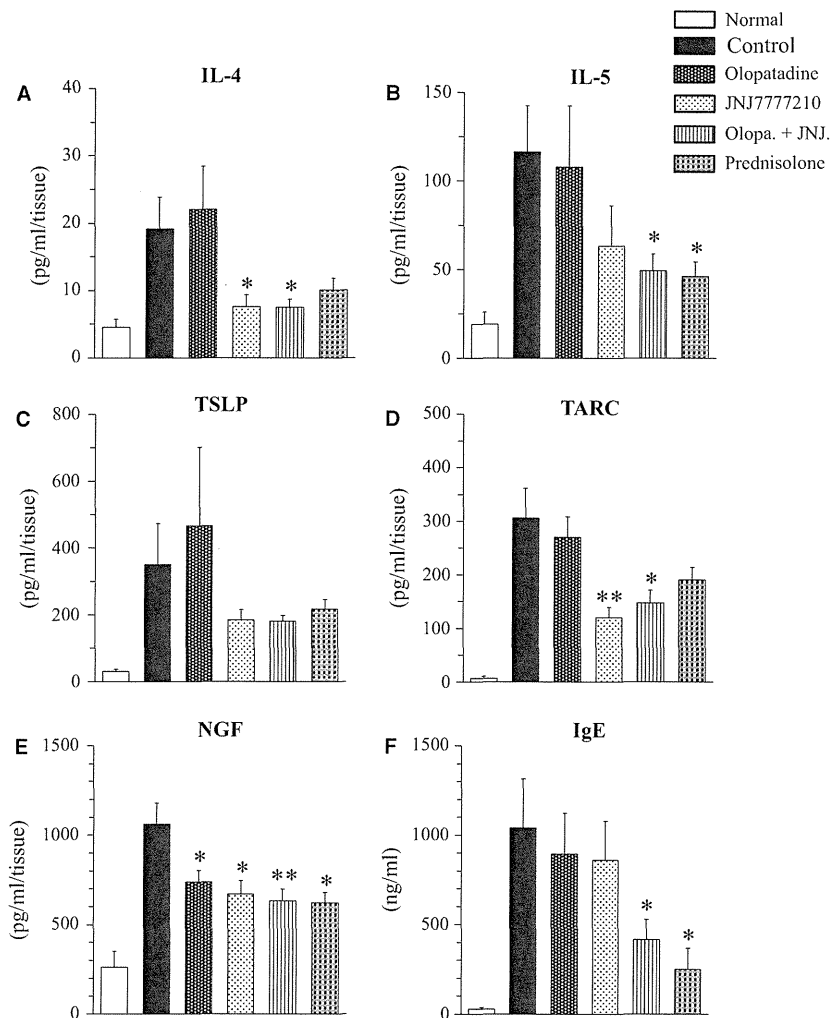


Figure 3 Effects of olopatadine and JNJ777120 on tissue cytokines and plasma IgE levels in picryl chloride (Picl)-induced chronic allergic dermatitis. Ten weeks after the sensitization, the levels of

cytokines (A–D), nerve growth factor (NGF) (E) in inflamed skin and total IgE in plasma (F) were determined. Statistical significance; * $P < 0.05$ and ** $P < 0.01$ vs control group ($n = 6–10$).

antagonist. In our study, we first clarified with the therapeutic efficacies in chronic dermatitis, administered both H1R and H4R antagonists. In our model of chronic dermatitis, a H4R antagonist suppressed the Picl-induced scratching behavior and, combined with a H1R antagonist, had an additive effect as reported in an acute inflammatory model by Rossbach et al. and chemical-induced pruritus model by Dunford et al. (16). As Thurmond et al. (25) suggested that both H1R and H4R are expressed on C-afferent fiber terminals, these drugs might inhibit directly the transmission of itching responses from the peripheral to central nervous system. In addition, we found that both olopatadine and JNJ777120 reduced the level of NGF in skin lesions. It has been reported that the level of NGF reflected the severity of itching and eruptions in AD (26, 27) and changed the correlation with clinical conditions in olopatadine-treated patients (27). Histamine also induced the production of NGF via H1R in human keratinocytes (28). Our findings suggested that H4R as well as H1R was involved in the

production of NGF, resulting in the increase in innervation in the epidermis.

Conversely, Sema3A expression was found to be decreased at the horn layer with immunohistological staining in the skin lesions of patients with AD (29). The decrease in the expression of Sema3A in the inflamed skin was also observed in our model (data not shown). In addition, decrease in Sema3A mRNA in the epidermis from *Dermatophagoides farinae*-induced chronic dermatitis in NC/Nga mice was recovered by olopatadine (30). In this study, we found that histamine decreased the level of Sema3A and olopatadine blocked this reduction in mouse keratinocytes. Because human keratinocytes also express H4R (31), the expression of Sema3A in human keratinocytes might possibly be regulated by H4R as well as H1R. To confirm this possibility, we have now begun studying it using mouse and human primary keratinocytes. These findings indicated that histamine acting via H1R and H4R induces the pruritus in chronic skin inflammation through

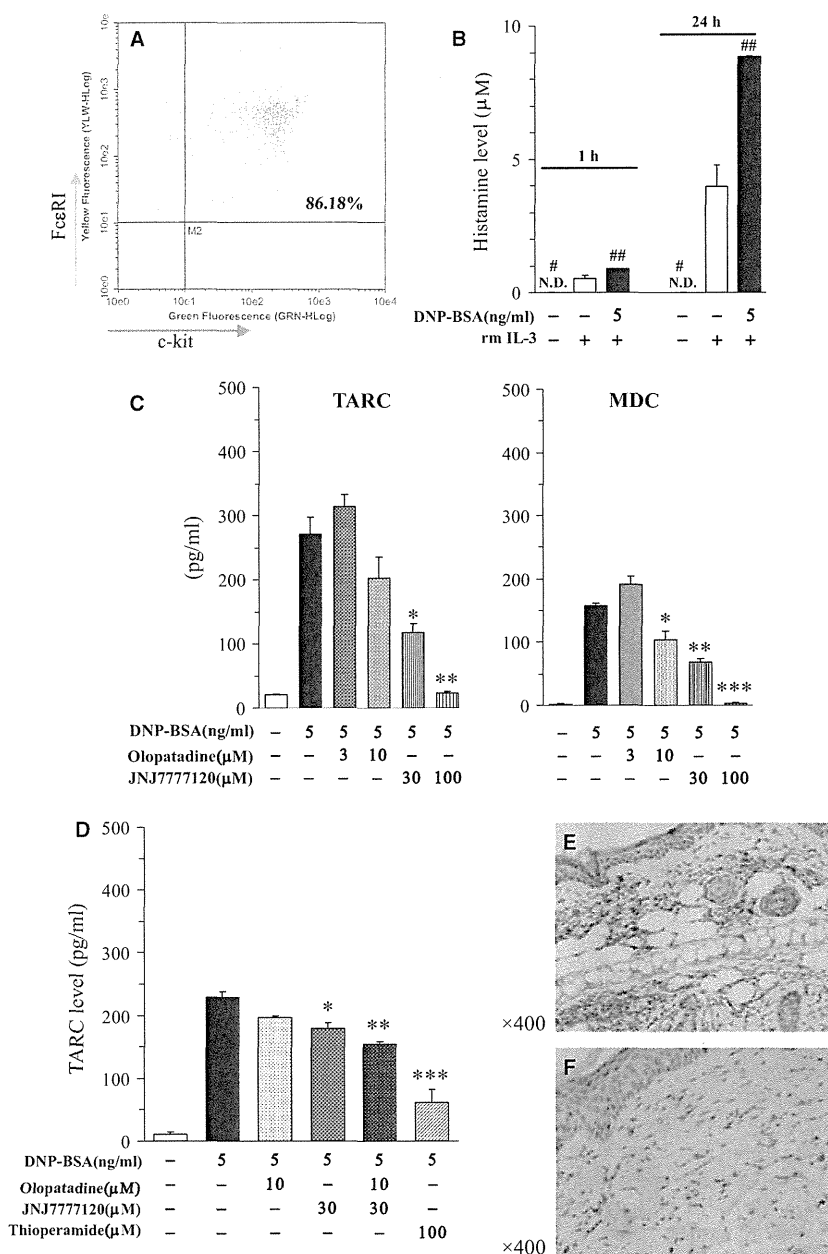


Figure 4 Effects of olopatadine and JNJ777120 on production of thymus and activation-regulated chemokine (TARC) and macrophage-derived chemokine (MDC) by antigen-stimulated bone marrow-derived mast cells (BMMC) and infiltration of CD4-positive cells in the skin lesions. (A) Bone marrow cells freshly prepared from NC/Nga mice were cultured with IL-3 (300 pg/ml) for 9 days and the expression of FcεRI and c-kit was confirmed by flow cytometry. (B) BMMC were primed overnight with 0.5 μg/ml of DNP IgE and then stimulated with DNP-BSA at the indicated concentrations. The level of histamine (1 and 24 h) in the supernatant

was determined. Statistical significance; #*P* < 0.05 and ##*P* < 0.01 vs unstimulated. (C, D) The cells were treated with olopatadine, JNJ777120 and thioperamide for 30 min, and then stimulated with DNP-BSA for 24 h. **P* < 0.05, ***P* < 0.01 and ****P* < 0.001 vs DNP-BSA stimulation. (E, F) Using the tissue specimens in Fig. 2, the CD4-positive T cells that had infiltrated the skin lesions in picryl chloride (PicI)-treated mice were revealed by immunohistological staining (control group, E; olopatadine and JNJ777120-administered group, F).

multiple mechanisms and that the combination of H1R and H4R antagonists has additive anti-pruritus effects.

Previously, we reported that the H3R/H4R antagonist thioperamide ameliorated ear swelling in mice with

TPA-modified hapten-induced allergic dermatitis, and in combination with the H1R antagonist pyrillamine suppressed the biphasic allergic response: the early phase in which vascular permeability is increased by the degranulation of